LBL-8005

TEMPERATURE-PROGRAMMED DESORPTION AND REACTION OF CO AND H_2 ON ALUMINA-SUPPORTED RUTHENIUM CATALYST

Gordon Gongngai Low
(M. S. thesis)

August 1978

Prepared for the U. S. Department of Energy
under Contract W-7405-ENG-48

LBL-8005

TEMPERATURE-PROGRAMMED DESORPTION AND REACTION OF CO AND H_2 ON ALUMINA-SUPPORTED RUTHENIUM CATALYST

Gordon Gongngai Low

Lawerence Berkeley Laboratory

Preceding page blank

TABLE OF CONTENTS

Preceding page blank

Temperature-Programmed Desorption and Reaction of CO and H_2 on Alumina-Supported Ruthenium Catalyst

Gordon G. Low
Materials and Molecular Research Division
Lawrence Berkeley Laboratory
University of California
Berkeley, California

ABSTRACT

The temperature-program desorption of CO and temperature-programmed reaction of CO in flowing H_2 has been studied on a 5 wt% Ru/Al_2O_3 catalyst. CO adsorbs molecularly on Ru/Al_2O_3 at room temperature. Two distinct CO desorption peaks were observed. The activation energies of desorption were calculated to be 27 and 37 kcal/mole.

Upon heating CO dissociates on Ru/Al_2O_3 at approximately 415°K to form CO_2 and carbon. The carbon remaining on the catalyst surface enhanced the strength of adsorption of CO, probably by donating electrons to increase the degree of back bonding of the adsorbed CO. The surface carbon reacted readily with H_2 at 303°K, forming CH_4 and small amounts of C_2H_6, whereas absorbed CO was inert to H_2 at this temperature. The surface carbon could easily be deactivated by heat treatment, and a very high temperature was required to remove the deactivated carbon from the catalyst surface with H_2.

These results strongly suggest that carbon is a reactive intermediate and that the dissociation of CO is a necessary step in methanation and Fischer-Tropsch synthesis.

Alexis T. Bell

I. Introduction and Literature Review

A. Introduction

The gasification of coal produces a carbon monoxide and hydrogen mixture which can be converted into methane, hydrocarbons, alcohols and a variety of basic chemicals. Although the synthesis of methane (methanation) and hydrocarbons (Fischer-Tropsch synthesis) from CO and H_2 has been studied for over 70 years, the basic mechanisms underlying these reactions are still the subject of active research. As a result little is known about the factors controlling catalysts activity or selectivity. The purpose of this work is to investigate the reactions of CO and H_2 over an alumina supported ruthenium catalyst. Ruthenium is chosen because it has high intrinsic activity compared to the other transition metal catalysts and because it yields mainly hydrocarbon products. Two investigative techniques, temperature-programmed desorption (TPD) and temperature-programmed reaction (TPR), are used to study the interaction and reaction of CO and H_2 on the Ru/Al_2O_3 catalyst. In the balance of this chapter a review is given of the TPD and TPR techniques and the studies on CO and H_2 chemisorption and reaction on Ru catalysts. Current proposals concerning the mechanisms of methanation and Fischer-Tropsch synthesis are also discussed.

B. Literature Review

1. Temperature-Programmed Desorption (TPD) and Temperature-Programmed Reaction (TPR)

Thermal desorption of gases from catalytic surfaces is a useful technique for the study of the details of bonding between an adsorbate and a catalyst. There are many reviews written on this subject [1-5]. One version of thermal desorption is flash filament desorption in which

the desorption of an adsorbate from an electrically heated "filament" is followed by monitoring the total pressure or the partial pressure of the adsorbate in an ultra-high vacuum system. This technique has been widely used in adsorption studies on single crystals, polycrystalline films, ribbons, and wires. Amenomiya and Cvetanović [6] extended the thermal desorption technique to the study of conventional supported catalyst by using a flow system. They coined the term temperature-programmed desorption (TPD). During a TPD experiment, the adsorbate is desorbed from the catalyst into a carrier gas by programmed heating. A linear heating schedule is most commonly used. The concentration of the adsorbate in the carrier gas stream is monitored as a function of the temperature of the catalyst, and the resulting concentration versus temperature plot is called a desorption spectrum.

A typical desorption spectrum is shown in Fig. 1. The rate of desorption is determined from the concentration of desorbed gas present in the gas phase. The number of peaks in a desorption spectrum is equal to the number of different types of adsorption sites on the catalyst surface, and the temperature at a desorption peak maximum is related to the activation energy of desorption for that adsorption site. Mathematical analysis of a first-order desorption process using certain simplifying assumptions results in Eq. (1) which relates the temperature at peak maximum to the heating rating and to the activation energy of desorption [5].

$$\ln \frac{T_m^2}{\beta} = \frac{E_d}{RT_m} + \ln \frac{E_d}{AR} \qquad (1)$$

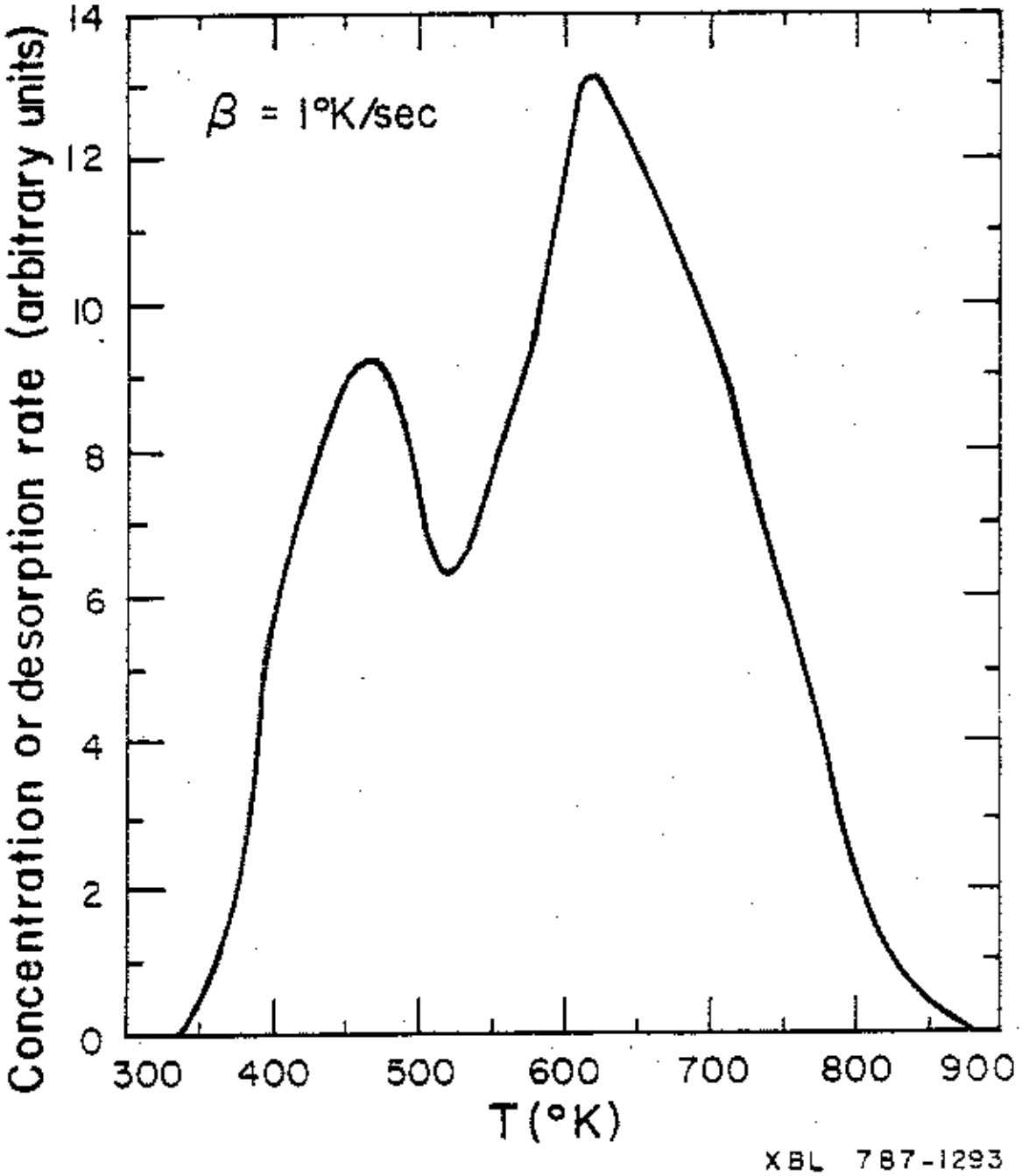

Figure 1. A typical desorption spectrum.

E_d - activation energy of desorption

T_m - temperature of peak maximum

β - linear heating rate

A - preexponential factor

The two basic assumptions used in the derivation of Eq. (1) are (i) that the catalyst surface is homogeneous, i.e. E_d is independent of coverage, and (ii) that desorption occurs at conditions where readsorption is negligible, i.e. high carrier gas flow rate.

If the second assumption is not valid, namely readsorption does occur freely, then an equation similar to Eq. (1) can be derived by assuming that equilibrium exists between the gas phase species and the surface species during desorption.

$$\ln\left(\frac{T_m^2}{\beta}\right) = \frac{\Delta H_d}{RT_m} + \ln\left[\frac{(1-\theta_m)^2\ V_s\ \Delta H_d}{F\ A^*\ R}\right] \qquad (2)$$

ΔH_d - differential heat of desorption

θ_m - coverage at peak maximum

V_s - solid volume of catalyst

F - carrier gas flow rate

A^* = exp ($\Delta S/R$) where ΔS is the entropy of desorption

For each desorption peak, a plot of ln (T_m^2/β) versus $1/T_m$ at different heating rates gives either E_d/R or $\Delta H_d/R$ as the slope of the

line, depending whether readsorption occurs or not during desorption. If adsorption is non-activated (i.e. the activation energy of adsorption, $E_a = 0$), the differential heat of desorption is equal to the activation energy for desorption ($\Delta H_d = E_d - E_a$). Under this condition Eq. (1) and Eq. (2) yield similar information.

In order to determine E_d or ΔH_d with a fair degree of accuracy, the heating rate must be varied by at least two orders of magnitude. Due to the experimental difficulties involved in doing so, a simplified form of Eq. (1) is commonly used [7] if readsorption is negligible at the desorption condition.

$$E_d/RT_m = \ln(A\ T_m/\beta) - 3.64 \qquad (3)$$

Using this equation E_d can be calculated from the data of one TPD experiment by assuming a typical value of 10^{13} sec^{-1} for the pre-exponential factor.

Although Eq. (1) was derived by assuming a first order desorption process, Lord and Kittleburger [8] have shown that Eq. (1) can also be used to calculate E_d for a second-order process if care were taken to start with the same initial coverage for each desorption experiment. An equation similar to Eq. (3) can be used for a second-order process.

$$E_d/RT_m = \ln\ (A_2\theta_o T_m/\beta) - 3.64 \qquad (4)$$

where θ_o is the initial coverage and A_2 is the preexponential for a second order process, typically equal to 10^{-2} cm^2/sec.

The utilization of Eq. (1-4) provides an easy means for determining the heat of desorption for the different adsorption sites on a catalyst surface. Also TPD experiments are useful for characterizing and identifying these different adsorption sites. However, care must be exercised in the interpretation of TPD spectra. The assumptions used in the derivation of Eq. (1) and (2) are often not valid at the desorption condition. Energetic non-homogeneity of the catalyst surface and adsorbate-adsorbate interaction can cause the activation energy to be coverage dependent. Also, increase in the mobility of the surface species as the temperature of the catalyst increases can lead to the interconversion of energetically different adsorbed species, thus adding to the complexity of interpreting the TPD results.

After identifying the different adsorption sites on a catalyst surface using the TPD technique, the activity of these sites for a catalytic reaction can be examined using the temperature-programmed reaction (TPR) technique. During a TPR experiment a gas is first adsorbed on the catalyst, but instead of using a carrier gas as in a TPD experiment, a gas which can react with the adsorbate is passed over the catalyst as the temperature of the catalyst is increased. The products of the reaction are monitored as a function of temperature. The temperature at which the products appear is an indication of the reactivity of the adsorbed species.

2. Mechanism of Methanation and Fischer-Tropsch Synthesis

Since Sabatier reported the synthesis of methane over a nickel catalyst in 1902, there has been a great deal of work done on the

synthesis of organic products from CO and H_2. The reaction of CO and H_2 to produce hydrocarbons is commonly referred to as Fischer-Tropsch synthesis. By the proper selection of catalyst and reaction conditions, it is possible to selectively produce a wide spectrum of products such as paraffins, olefins, alcohols, ketones, aldehydes, and fatty acids. Many excellent reviews of the history, kinetics, thermodynamics, reaction mechanisms, and technological developments pertaining to Fischer-Tropsch synthesis have been published [9-19]; therefore, a comprehensive review on this subject will not be given here. This review will be concerned mainly with studies of the interaction and reaction of CO and H_2 on Ru, and a major emphasis will be placed on the proposed mechanisms of methanation and Fischer-Tropsch synthesis.

One of the earliest mechanisms proposed for the $CO-H_2$ synthesis reaction was the carbide theory of Fischer and Tropsch [19]. This theory postulated that the synthesis reaction is initiated by the dissociation of carbon monoxide on the catalyst surface to produce a surface carbide. The surface carbide then reacts with adsorbed hydrogen to form a CH_2 intermediate which can be hydrogenated to form methane or undergo polymerization to form higher molecular weight hydrocarbons. The mechanism can be represented by the following steps.

$$CO_{(g)} + M \longrightarrow M-CO \qquad (1)$$

$$H_{2(g)} + 2M \longrightarrow 2\ H-M \qquad (2)$$

$$M-CO + M \longrightarrow M-C + M-O \qquad (3)$$

$$M-O + H-M \longrightarrow M-OH \qquad (4)$$

$$M-OH + H-M \longrightarrow H_2O + 2M \qquad (5)$$

$$M-C \xrightarrow{2\ H-M} M=CH_2 \xrightarrow{2\ H-M} CH_4 + M \qquad (6)$$

$$M{=}CH_2 + M{=}CH_2 \xrightarrow{H-M} M{-}CH_2{-}CH_3 + M \qquad (7)$$

$$M{=}CH_2 + M{-}CH_2{-}R \xrightarrow{H-M} \text{paraffins, olefins} \qquad (8)$$

$$M{-}CH_2{-}R + M{-}OH \xrightarrow{H-M} \text{oxygenated hydrocarbons} \qquad (9)$$

Steps (7) and (8) are the chain-growth steps, and step (9) is proposed in order to explain the formation of oxygenated hydrocarbons. It has also been proposed that a possible mechanism for chain growth is the direct insertion of adsorbed CO into the $M{=}CH_2$ intermediate [20]. If this occurs then steps (4), (5), and (7-9) can be replaced by

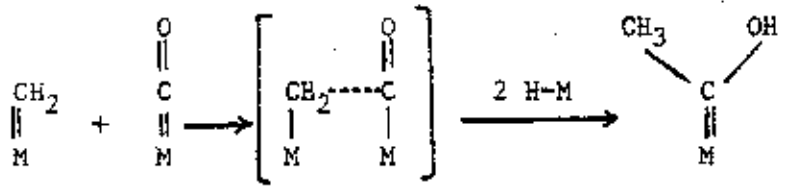

(10)

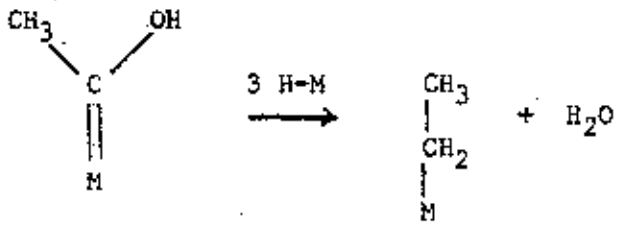

(11)

$$M{-}CH_2{-}R \xrightarrow{H-M} \text{paraffins, olefins} \qquad (12)$$

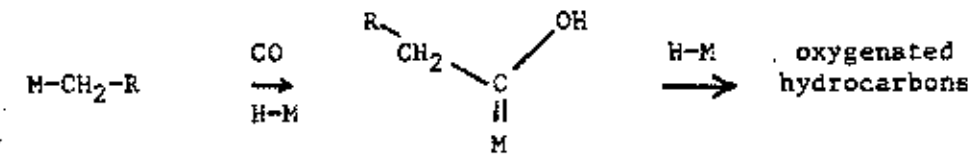

(13)

The carbide theory was later rejected because it failed to explain the synthesis reaction over the iron group (Fe, Co, Ni) catalyst. Tracer studies with ^{14}C [21-23] and kinetic studies [24-29] showed that the carbide could not be the intermediate in the synthesis reaction. A summary of the reasons for the rejection of the carbide theory was discussed by Pichler [12] and by Kini and Lahiri [30].

Storch, Golumbic, and Anderson [16] proposed a different mechanism involving a hydrogenated CO intermediate, an enol. The enol intermediate can be hydrogenated to form either methane or methanol, or it can undergo a condensation reaction to form higher molecular weight hydrocarbons. This mechanism can be represented by the following steps.

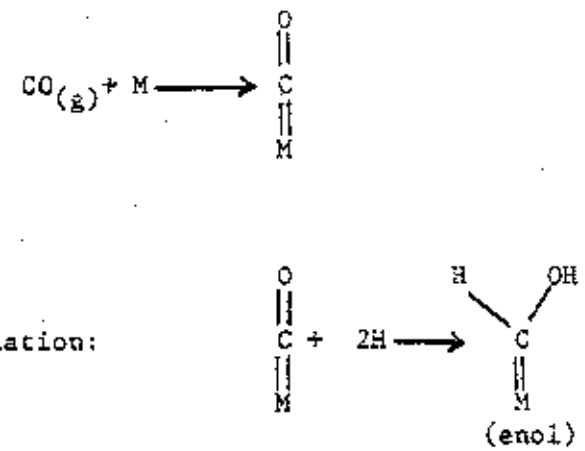

(1)

Chain initiation:

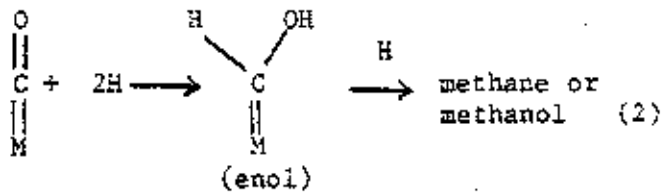

(2)

Chain growth:

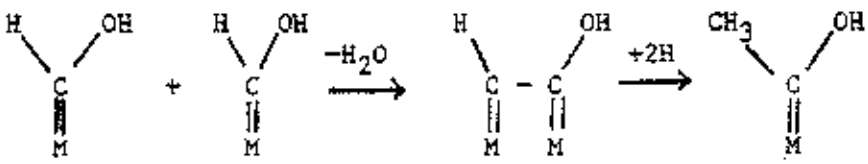

(3)

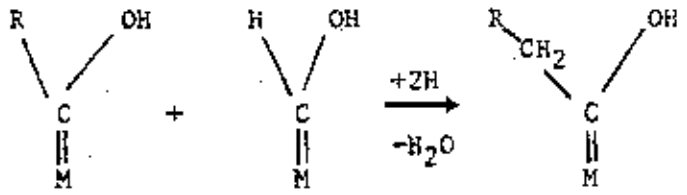

(4)

Chain termination:

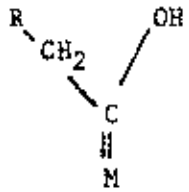

$\xrightarrow{2H}$ oxygenated hydrocarbons (5)

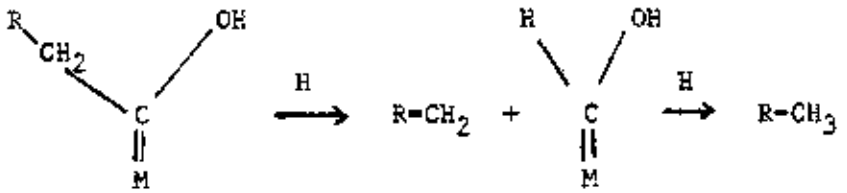

(6)

This mechanism was widely accepted after its introduction, but there was very little direct evidence to prove the existence of an enol intermediate on catalyst surfaces. Bhyholder and Neff [31] observed O-H and C-H infrared bands on Fe/SiO_2 exposed to CO and H_2. They assumed that these bands were due to the presence of an enol intermediate. Other indirect evidence which seemed to support the existence of an enol intermediate was obtained from studies of the coadsorption of CO and H_2. It was found that, irrespective of the initial H_2/CO ratio of a gas mixture exposed to an Fe catalyst, a 1/1 H_2/CO mixture was desorbed from the catalyst [32]. This observation was explained by postulating the existence of an enol type surface complex. A recent study by Matsumoto and Bennett [33] presented similar arguments for the existence of an enol intermediate. They observed that when a reaction mixture of CO and

H_2 flowing over a promoted Fe catalyst at 523°K was suddenly changed to flowing He, only H_2O was detected in the He stream. They proposed that H_2O was formed via the reaction,

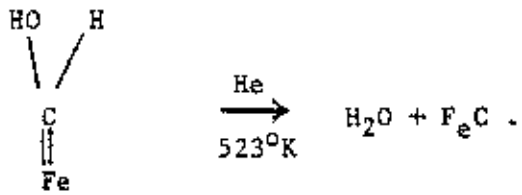

The carbide remaining on the catalyst surface was found to be less reactive toward H_2 than CO.

Due to the renewed interest in methanation and Fischer-Tropsch synthesis, there has been a large investigative effort directed toward the identification of the reaction mechanism. Recent studies on the mechanism of methanation have revived the carbide theory. Wentrek, Wood, and Wise [34] pulsed a known volume of CO over a Ni/Al_2O_3 catalyst at 553°K. They found that some of the adsorbed CO dissociated into carbon and CO_2 via the reaction ($2\ CO \rightarrow C + CO_2$). When this same catalyst was pulsed with H_2 at 553°K, the methane produced was almost exactly equal to the amount of carbon deposited on the catalyst surface. No correlation was found between the amount of chemisorbed CO and the amount of methane produced. When the catalyst was heated at 723°K for 10 min after carbon deposition at 553°K, deactivation of the carbon was oserved. The authors distinguished the reactive form of carbon as carbidic carbon and the unreactive form as graphitic carbon. It was probably the latter which investigators in the past [23-25] had found to be unreactive. In a later study McCarty, Wentrek, and Wise [38] found that the carbon deposited on a Ru/Al_2O_3 catalyst was reactive in H_2 to form CH_4 below room temperature, but undissociated CO adsorbed on the catalyst was inert to H_2 at room temperature.

Similar experiments were performed by Rabo, Rish, and Poustma [20] using Ru, Ni, Co, and Pd supported on silica. The adsorption of CO was nondissociative on these catalyst at room temperature, and the chemisorbed CO did not react with H_2 at this temperature. But when carbon was first deposited on the Ru, Ni, or Co catalyst by CO adsorption at 573°K and subsequently cooled to room temperature, methane was produced when the H_2 was pulsed over the catalyst at room temperature. CO did not dissociate on the Pd catalyst at 573°K, and the chemisorbed CO (adsorbed at 573°K) was inert to H_2 at room temperature. These results are consistent with the fact that Ru, Ni, and Co are excellent methanation catalysts, while Pd is only slightly active in methanation, but it is a good catalyst for methanol synthesis under moderate pressure. Therefore, it was concluded that the dissociation of CO leads to the formation of methane, and the direct hydrogenation of undissociated CO leads to the formation of methanol.

Araki and Ponec [36] also examined the reactivity of the carbon deposited on a Ni film. ^{13}CO was exposed to a clean Ni film at 573°K for 30 min to deposit a layer of carbon on its surface. The chemisorbed ^{13}CO was then pumped away, leaving only the surface carbon ^{13}C, then a reaction mixture of ^{12}CO and H_2 (5/1) was introduced at 523°K. The formation of $^{13}CH_4$, $^{12}CH_4$, $^{13}CO_2$, and $^{12}CO_2$ was monitored as a function of time. At first only $^{13}CH_4$ was observed. The formation of $^{12}CH_4$ and $^{12}CO_2$ was accompanied by an induction period of approximately 25 min and $^{13}CO_2$ was not detected. These facts clearly demonstrated that the surface carbide was the intermediate in the methanation reaction.

3. Studies of CO and H_2 Reaction and Interactions on Ruthenium

Ru is an excellent methanation catalyst at atmospheric pressure. It also has the unique ability to synthesize high molecular weight paraffinic waxes at high pressure. Table 1 summarizes the results of the kinetic studies on the hydrogenation of CO over different Ru catalysts [17]. These studies generally show that CO inhibits the reaction while H_2 has a positive-order effect on the reaction rate.

Vannice [37] compared the turnover numbers for the methanation reaction for the Group VIII transiton metals and found that Ru has the highest activity (see Table 2). Dalla Betta et al. [38] measured the initial methanation activity of supported Ru and Ni catalyst and found that Ni was twice as active as Ru at 553°K. However, a later study by the same authors [39] showed that Ru, Ni, and Re catalyst have similar steady state methanation activity.

Dalla Betta and Shelef [40] performed an infrared study of the hydrogenetion of CO. They found that the adsorption band for CO in the presence of H_2 was very strong. The catalyst surface was almost saturated by adsorbed CO during the reaction at temperatures from 353°K to 523°K. No evidence for an enol type reaction intermediate was detected. However infrared bands attributable to hydrocarbons and formates species were observed. Isotopic-exchange experiments indicated that these species were inert and were adsorbed on the alumina support. At high reaction temperature the metal surface was altered, possibly due to carbon deposition, and an adsorbed CO exhibiting a much lower stretching frequency and a greatly reduced intensity was observed. The catalytic activity was also reduced.

Table 1. Empirical Kinetic Expressions for the Hydrogenation of CO on Ru [17].

Catalyst	Rate Expression	Reaction Conditions					
		T(°K)	P_{H_2} (kpa)	P_{co} (kpa)	P_{total} (kpa)	H_2/CO	E_{CH_4} (kJ/mole)
1.5% Ru/Al_2O_3	$r_{CH_4} = A \exp(-E/RT) P_{H_2}^{1.8} P_{co}^{-1.1}$	473-613	57.8	19.2	77	3	100
9% Ru/Al_2O_3	$r_{CH_4} = A \exp(-E/RT) P_{H_2}^{1.6} P_{co}^{-0.6}$	478-503	77.2	25.8	103	3	101
Ru/Al_2O_3	$r_{CH_4} = kP_{H_2}^{1.33} P_{co}^{-0.13}$	503-543	1631	527	2168	3.04	-
Ru/Al_2O_3	$r_{CH_4} = kP_{co}$	468-548	101	0.054	101	1869	-
Ru metal	$r_{CH_4} = kp_{H_2}^2$	293-443	2.0-5.1	1.3-13.2	1.0-16.2	38	-

Table 2. Specific Methanation Activity of Group VIII Transition Metals [37]

Metal	(Turnover no. @ 548°K × 10^3)
Ru	181
Fe	57
Ni	32
Co	20
Rh	13
Pd	12
Pt	2.7
Ir	1.8

Kraemer and Menzel [41] examined the interaction of CO and H_2 on a Ru field emitter. They found that a saturated layer of CO at 300°K did not adsorb any H_2, but a saturated layer of the H_2 was very effectively replaced by CO. During the displacement of H_2 by CO, a mixed layer was formed and a change in the work function of the surface was detected, which suggests the existence of a complex. This complex was more strongly bonded to the surface than CO or H_2 alone. Goodman et al. [42] observed similar interactions between CO and H_2 adsorbed on a Ru (110) surface. The addition of CO to a saturated H_2 layer increased the desorption temperature of H_2 by approximately 45°K.

4. Studies of CO and H_2 adsorption on Ruthenium

In order to fully understand the mechanistic steps involved in methanation and Fischer-Tropsch synthesis, it is essential that the adsorption of CO and H_2 on catalyst surface is well understood. This section is devoted to a review of CO and H_2 chemisorption on Ru surfaces.

A model for the bonding of CO on transition metal is shown in Fig. 2 [43]. The electron pair from the 3σ orbital of the carbon atom is donated into the vacant d orbits of the metal atom. This bond is very weak because the donor ability (Lewis basicity) of the CO molecule is extremely small, so the metal-carbon bond is stabilized by back donation of electrons from the filled d orbitals of the metal into the vacant antibonding orbitals of the CO molecule. Since the electrons are donated into the antibonding orbitals of the CO molecule, A weakening the CO bond would be expected. The ability of the CO molecule to bond to the transition metal depends on the availability of filled and vacant d orbitals with the correct symmetry and range of energies. A CO molecule can form bonds with one metal atom,

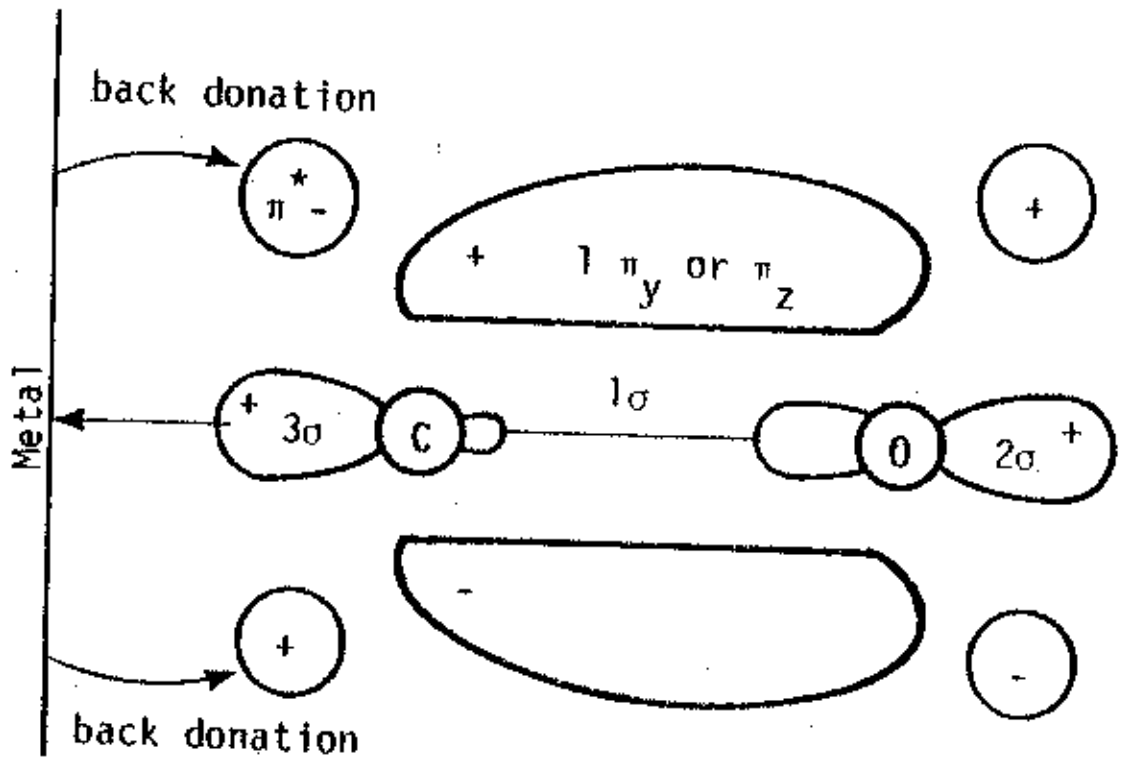

XBL 787-1309

Figure 2. Molecular-orbited description of CO adsorption on transition metal.

two metal atoms, and even three or more metal atoms if a favorable energy configuration can be achieved.

Quantitative measurements of CO adsorption on Ru have been performed by a number of authors [44-46]. H_2 chemisorption and BET surface area determination (for powdered metal only) were used to determine the number of surface Ru atoms. The ratio of the number of adsorbed CO molecules to the total number of surface Ru atoms ranges from 0.6 to 3.8. The adsorption stoichiometries were explained by postulating the existence of bridge-bonded CO and multiple adsorption of CO on a Ru atom.

Infrared spectroscopy is a common technique used to study the structure of CO adsorbed on metals. A number of infrared studies on the adsorption of CO on Ru surfaces has been published. Table 3 summarizes the results. The earliest study of CO adsorption on Ru was by Lynds [47]. He reported two bands at 2151 cm^{-1} and 2083 cm^{-1} for Ru/Al_2O_3 and two bands at 2125 cm^{-1} and 2060 cm^{-1} for Ru/SiO_2. Guerra and Schulman [48] found two broad bands at 2010-1990 cm^{-1} and 1970-1870 cm^{-1} for CO adsorbed on Ru/SiO_2. They assigned the high frequency band to linearly adsorbed CO (Ru-CO) and the low frequency band to bridge-bonded CO (Ru_2-CO). Kobayashi and Shirasaki [49] assigned bands observed at 2040 cm^{-1} and 1980 cm^{-1} to $Ru(CO)_2$ and $Ru(CO)_3$ respectively for CO adsorption on a Ru/SiO_2 catalyst. These structural assignments were based on the infrared spectra of Ru carbonyl clusters and the results of CO chemisorption experiments which suggested that multiple CO adsorption occurs on Ru surfaces.

Table 3. Infrared Study of CO on Ru

Form of Ru	Bands (cm^{-1}) HF	MF	LF	Structural assignments	References
Ru/Al_2O_3	2151	2083	---	----------	[47]
Ru/Al_2O_3	2133-2148	2070-2086	2028-2092	CO adsorbed on different coordination sites	[46]
Ru/SiO_2	2125	2060	----	----------	[47]
Ru/SiO_2	---	---	2010-1990 1970-1870	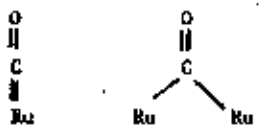	[48]
Ru/SiO_2	---	---	2040, 1980	$Ru-(CO)_2$ $Ru-(CO)_3$	[49]
Ru/SiO_2 (reduced)	---	---	2040		[51]
Ru/SiO_2 (fully oxidized)	2130	2070	---	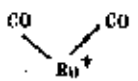	[51]
Ru/SiO_2 (reduced)	2150 (weak)	2080 (weak)	2030 (strong)	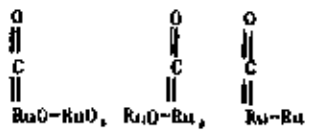	[50]
Ru/SiO_2 (partially oxidized)	2135 (medium intensity)	2080 (strong)	2010 (medium intensity)		[50]

A recent infrared study by Dalla Betta [46] on CO chemisorption on Ru/Al_2O_3 samples having different crystalline sizes showed some interesting results. Only one band was observed at 2028 cm^{-1} for CO adsorbed on Ru/Al_2O_3 with average metal crystallite size greater than 91 Å. However, three bands at 2028-2092 cm^{-1}, 2070-2086 cm^{-1}, and 2133-2148 cm^{-1} were observed when CO was adsorbed on Ru/Al_2O_3 with average metal crystallite size less than 60 Å. Comparison of CO and H_2 adsorption revealed CO/H ratios as high as 3.8 on Ru particle of 11 Å, implying multiple adsorption of CO on low coordination sites. Based on this evidence Dalla Betta concluded that the observed bands were due to CO adsorption on different coordination sites.

Brown and Gonzales [50] conducted infrared studies on the adsorption of CO on reduced and oxidized Ru/SiO_2. The intensities of the bands at 2030 cm^{-1}, 2080 cm^{-1}, and 2135-2150 cm^{-1} were dependent on the degree of oxidization of the Ru/SiO_2. They concluded that the observed bands were due to linearly adsorbed CO perturbed to a different degree by an oxygen atom. The following structures were proposed:

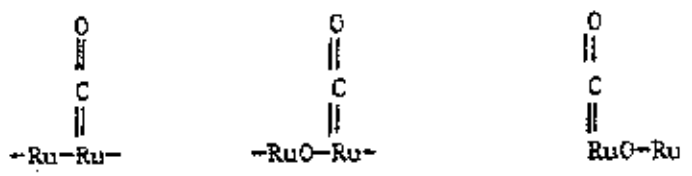

2030 cm^{-1} 2080 cm^{-1} 2135-2152 cm^{-1}

Davydov and Bell [51] also studied the adsorption of CO on oxidized and reduced samples of Ru/SiO_2. They found only one band at 2040cm^{-1} for CO adsorbed on fully reduced Ru/SiO_2, to which they assigned the structure of Ru-CO. The bands observed on fully oxidized Ru/SiO_2 at 2130 cm^{-1} and 2070 cm^{-1} were assigned the structure $Ru^{+}-(CO)_2$.

Madey and Menzel [52] used a combination of surface techniques, LEED, Auger, Kelvin probe contact potential changes, and flash desorption to study the adsorption of CO on Ru (001). Two binding states of CO were identified by flash desorption from a saturated Ru surface, but only the higher temperature peak was observed at low CO coverage. The LEED pattern indicated a $(\sqrt{3} \times \sqrt{3})$ structure at low CO coverage, but this ordered pattern decreased in intensity as CO coverage increased beyond 1/3 of a monolayer. This evidence seems to indicate that the two binding states at high coverage arises from the repulsive interactions between neighbors. It was found that bombardment by LEED electron beam changed the $(\sqrt{3} \times \sqrt{3})$ pattern to a (2×2) pattern. This observation was later studied in more detail by Fuggle et al. [53] using flash desorption, UPS, XPS, and XAES techniques. Slow electron bombardment of adsorbed CO on Ru (001) gave rise to a new peak in the flash desorption spectrum. This new peak desorbed at a higher temperature than the two CO peaks previously identified. XPS and UPS results seemed to show that this new binding state was dissociated CO occupying two surface sites. It is of interest to note that this new binding state of CO cannot be obtained even by exposing the Ru surface to 10^{-5} torr of CO at 490°K for 20 min.

Goodman et al. [42] studied CO adsorption on a Ru (110) surface having a high density of kinked atomic rows. Ony one peak was observed during the flash desorption of CO at different coverages. At low CO coverage no ordered LEED pattern was observed, but at high coverage an ordered structure appeared and persisted to saturation. UPS studies showed no detectable change in the molecular-orbital structure of CO

between low and high coverage; therefore it was concluded that only one CO binding state exists on Ru (110). Auger spectra taken of the surface showed no surface carbon species on the Ru(110) surface after exposure to 10^{-3} torr of CO at 630°K for 30 min. Also no detectable CH_4 was formed in a 4/1 H_2/CO mixture at 10^{-3} torr in the temperature range of 300-1400°K. Thermodynamic calculations showed that this is due to kinetic limitation.

Reed et al.[54] studied CO adsorption on a Ru (101) surface using LEED, Auger, and thermal desorption. Two poorly resolved peaks were evident in the flash desorption spectrum at all CO coverages; therefore the authors concluded that CO adsorbs on two distinct surface sites on Ru(101). An ordered LEED pattern was observed at low CO coverage and reached a maximum degree of perfection at saturation coverage. Dissociation of CO was not detected after exposing the surface to 10^{-7} torr of CO for 5 min in the temperature range of 373-1073°K. However, bombardment by the LEED electron beam did cause dissociation. Adsorption on carbon contaminated surface shifted the thermal desorption peaks to a lower temperature and a new high temperature shoulder appeared at high CO coverage.

Using the same surface techniques as Reed et al. [54], Ku et al. [55] studied the adsorption of CO on a Ru(100) surface. They observed two desorption peaks at high CO coverage and only the high temperature peak was observed at low CO coverage. No ordered LEED pattern for CO adsorption was observed.

McCarty et al. [35] recently studied the desorption of CO from a 1.5 wt % Ru/Al_2O_3 catalyst and observed three desorption peaks. This is the only result available for CO desorption from a supported Ru catalyst. Table 4 summarizes the results of the studies on the thermal desorption of CO from Ru. The values of the activation energy of desorption were calculated using Eq. (3). The results from this work which will be presented in greater detail in the latter sections are also shown in Table 4.

The adsorption of H_2 on Ru will be briefly discussed here. It is well known that H_2 adsorbs dissociatively on many transition metals. H_2 chemisorption has been widely used as a tool in the determination of metal surface area. Dalla Betta [56] studied the chemisorption of H_2 on powdered Ru. The adsorption of H_2 was found to be slow at room temperature; approximately 200 min was needed to attain equilibrium. The particle size of the Ru powder determined by electron microscopy was consistent with the particle size calculated from the results of H_2 chemisorption experiments by assuming one hydrogen atom absorbs on one surface Ru atom.

Using the BET method to determine the surfce area of a powdered Ru sample, Taylor [57] found that the ratio of adsorbed hydrogen atoms to surface Ru atoms ($H/Ru_{(s)}$) to be 1.1. Identical H_2 uptakes on Ru were obtained by extrapolating the 23°C and 100°C isotherm to

Table 4. Thermal Desorption Study of CO on Ru

Form of Ru studied	T_m (°K)	Heating rate (°K/sec)	E_d (kcal/mole)*			Reference
Ru(100)	403, 495-513 ---	8	24.4	30.1	--	[55]
Ru(001)	400, 450-465 ---	11	23.5	28	--	[52]
Ru(001)	410, 470 550-600	5	25	29	34-37	[53]
Ru(101)	440, 485-520 ---	30	25	28	—	[54]
Ru(110)	350-550	0.05	24-39			[42]
1.5 wt% Ru/Al_2O_3	455, 570, 630	1.0	29	37	41**	[35]
5 wt % Ru/Al_2O_3	440, 575, poorly resolved	1.1	27	37	--	present work

*Calculated using Eq. (3), $E_d/RT_m = \ln(AT_m/\beta) - 3.64$, with $A = 10^{13}$ sec^{-1}.

**The E_d values are calculated by us using the TPD data of McCarty et al. [35].

zero pressure and therefore the same $H/Ru_{(s)}$ stoichiometry of 1/1 holds at both temperatures. Thus surface area determination of Ru catalyst by H_2 chemisorption can be carried out at 100°C where adsorption equilibrium can be reached in approximately 30 min.

Goodman et al. [42] studied the flash desorption of H_2 from a Ru (110) surface. H_2 adsorption was carried out at 300°K and only one desorption peak at 353°K was observed. The desorption characteristics resembled a first order desorption process. The activation energy of desorption E_d was calculated to be 17.5 kcal/mole using a preexponential factor of 10^{12} sec^{-1}. Analysis of the desorption products obtained from the adsorption of 1/1 H_2/D_2 mixture revealed that hydrogen was adsorbed atomically.

II. Experiment

A. Experimental Apparatus

A diagram of the experimental apparatus is shown in Fig. 3. The apparatus consists of a flow system, a reactor, and a high vacuum system which houses the quadrupole mass spectrometer.

The flow system was designed so that it was possible to provide either a continuous flow or a pulse of CO, H_2, H_e, or a mixture of these gases to the reactor. This was accomplished by using two 6-way valves in series. The volume of each pulse was approximately 1.5 cc. The gas flow rate was controlled by adjusting the needle valves located upstream and downstream from the rotometers. Mercury monometers were used to monitor the pressure at which the flow rate was measured. The flow system was helium-leak tested to insure that air could not enter the system and thereby contaminate the catalyst. The entire system could be evacuated with a mechanical pump to facilitate changing from one gas to another during an experiment.

The gases used in the experiment were purified by using appropriate cold traps. Hydrogen (99.999% pure) from the gas cylinder first goes through an Engelhard Deoxo Hydrogen Purifier to convert the traces of O_2 to water. The water was then trapped out by molecular sieves kept at liquid nitrogen temperature. Helium (99.998% pure) was also purified by using a liquid nitrogen trap filled with molecular sieves. Carbon monoxide (99.8% pure) was sent through a bed of potassium hydroxide pellets kept at dry ice temperature to remove CO_2 and metal carbonyls.

A detailed drawing of the reactor and heater is shown in Fig. 4. The reactor is a 21 cm long, 6 mm o.d. quartz tube with a 12 mm o.d.

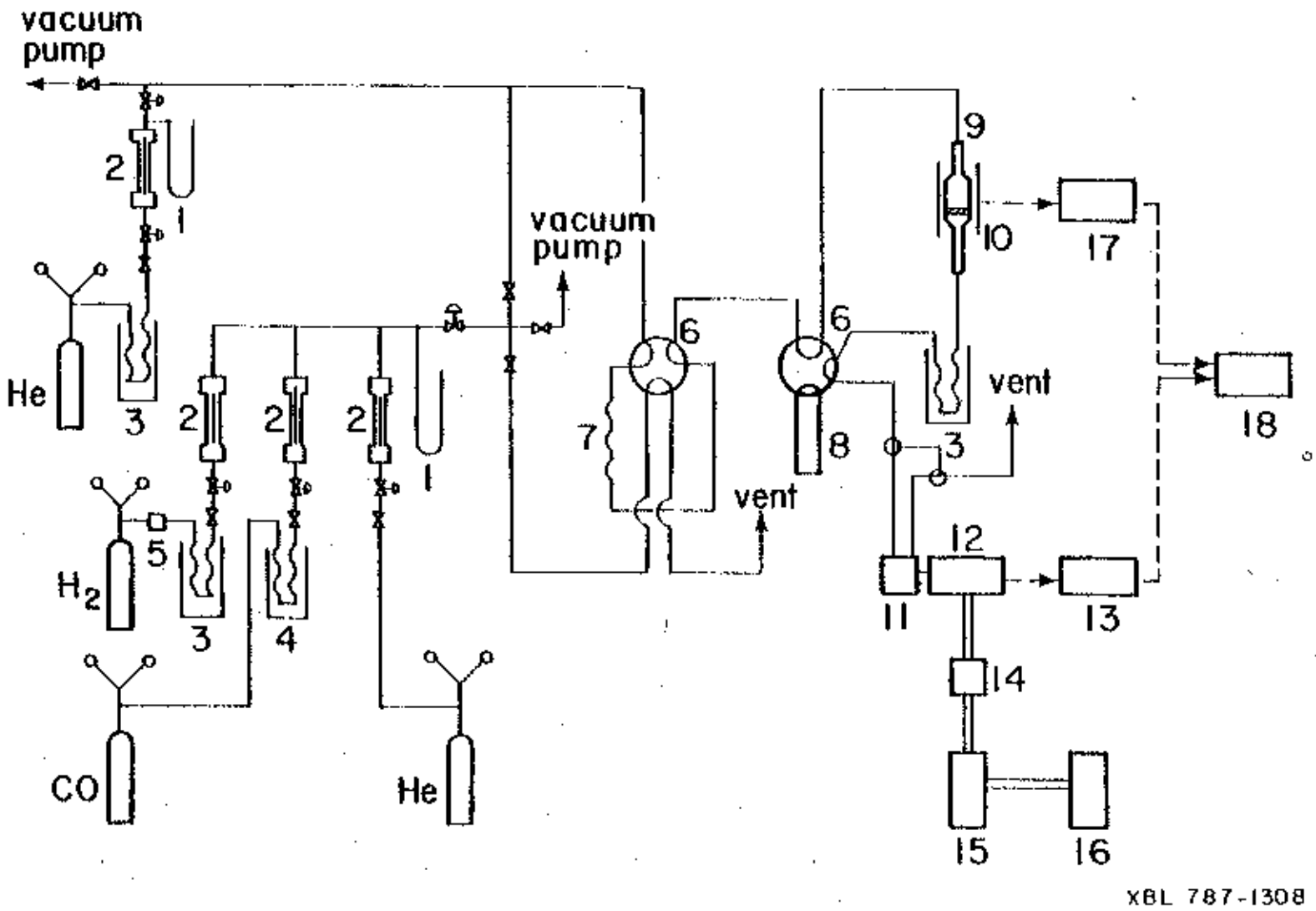

Figure 3. Experimental apparatus.

List of Equipment

1. Hg manometer
2. Rotometer
3. LN_2 cold trap
4. Dry ice cold trap
5. Catalytic hydrogen purifier
6. Six-way valve
7. Sample loop fot pulse adsorption
8. Reactor by-pass
9. Reactor
10. Heater
11. Leak valve
12. Mass spectrometer probe
13. Mass spectrometer electronics
14. LN_2 cold trap
15. Oil diffusion
16. Mechanical pump
17. Temperature programmer
18. Two-pen recorder

a. Catalyst sample

b. Quartz reactor tube.

c. Thermocouple for temperature readout.

d. Thermocouple for temperature control

e. Heater

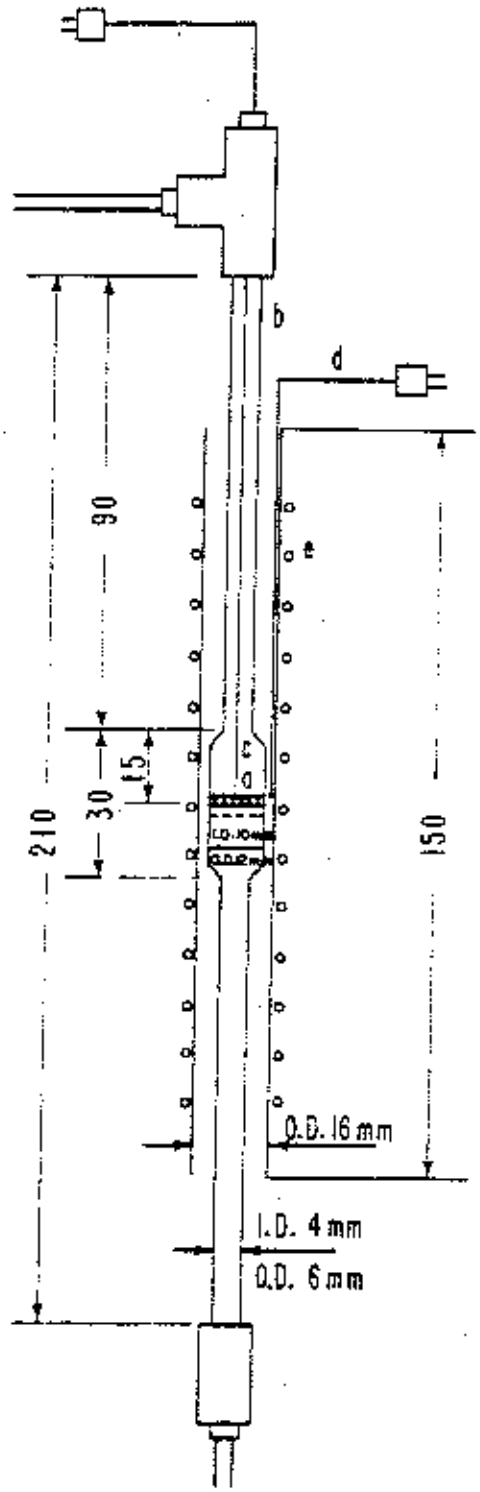

XBL785-826

Figure 4. Schematic of reactor and heater.

bulb-shaped mid-section. A quartz fritted disc, used to support the catalyst sample, was fused into this section of the reactor. The reactor could be removed from the flow system by disconnecting the top and bottom compression o-ring fittings (Cajon). The heater was constructed in the following fashion. Two pieces of nichrome wires with a resistance of 6.5 ohms each were wound on a 1.9 cm o.d. quartz tube such that the two coils were located one above the other. These two coils were then connected in parallel to the power supply.

A temperature programmer was used to power the heater. This device was constructed in the College of Chemistry electronics shop (drawing number 827A1). It could be used to maintain the reactor at constant temperature, or be programmed to heat up the reactor at a constant heating rate from an initial to a final temperature. The following parameters could be set: (i) initial temperature, (ii) final temperature, and (iii) heating rate. Temperature control was achieved by pulsing the power to the heater. Depending on the heating rate, the size of the power pulse can be adjusted. This added feature reduced the temperature ripples on the linear heating curves for the lower heating rates. The heating rate could be varied from 0.03°K/sec to 1.0°K/sec. The reactor could be heated to a maximum temperature of 1100°K. The temperature programmer was rated at a maximum output power of 320 watts (40 volts d.c. and 8 amp.).

Experimentally it was found that the rate of heating and temperature control of the reactor were best achieved by placing the temperature-control thermocouple for the temperature programmer nearest to the heating

coils. A different thermocouple, inserted through a tee, was used to monitor the temperature of the catalyst. The signal from this thermocouple was recorded by one pen of a Leeds and Northrup Speedomax W/L Two-Pen Recorder.

The gas leaving the reactor was analyzed by a UTI model 100C quadrupole mass spectrometer. The probe of the mass spectrometer was housed in a vacuum chamber. A Granville-Phillips series 203 variable leak valve was used to allow a constant leak of the gas leaving the reactor into the vacuum chamber. The leak opening was adjusted such that the total pressure inside the chamber was 2.0×10^{-6} torr with a continuous leak of pure He. An ultimate vacuum of 5×10^{-9} torr could be achieved by using a 4-inch oil diffusion pump (VHS series, National Research Corporation). Total system pressure cold be measured directly by the mass spectrometer. The mass spectrometer could be programmed to lock in on four different masses. By rapid manual switching from one program to another, it was possible to monitor up to four different species at one time. The signal from the mass spectrometer was recorded by the second pen of the two-pen recorder.

B. Experimental Procedures

The experiments can be divided into three main groups: temperature-programmed desorption (TPD) of preadsorbed CO, temperature-programmed reaction (TPR) of preadsorbed CO, and temperature-programmed reaction of continuously flowing gas mixtures. In order to eliminate the effect of carbon build up and catalyst sintering on the experimental results, fresh catalyst samples were used for each experimental run. Twenty five milligrams of the Ru/Al_2O_3 catalyst was placed in the reactor and reduced in flowing H_2 (1 atm) at 723°K for at least 9 hrs (Exceptions were

the TPR experiments designed to examine the effect of aging on the reactivity of the carbon deposit, where a reduction time of 2 hrs at 673°K was used). At the end of the reduction period, He was introduced to sweep away the H_2 and the catalyst was heated up from 723°K to 973°K at a rate of 1°K/sec in order to desorb any adsorbed H_2. The catalyst was then cooled to the adsorption temperature in flowing He.

For the TPD experiments CO was pulsed ten times over the catalyst in a period of 5 min. The catalyst was then swept with He at the adsorption temperature for an additional 5 min and finally cooled to 303°K in approximately 15 min. Next, the He flow rate was adjusted to 30 cc/min (STP), and the catalyst sample was heated from 303°K to 973°K at the selected heating rate. During the heating period the concentrations of CO (mass 28) and CO_2 (mass 44) in the He stream were monitored as a function of temperature.

A nitrogen cold trap down stream from the reactor was used to trap out the CO_2 formed by the disproportionation of CO during pulse adsorption. After pulse adsorption was completed, the cold trap was warmed up, and the amount of CO_2 trapped was measured with the mass spectrometer.

The TPR of CO preadsorbed by the pulse method followed the same catalyst reduction and adsorption procedures described above. After adsorption of CO, the catalyst was cooled to 303°K in flowing He. The 6-way valve was then switched to the by-pass mode, isolating the reactor from the flow system. The He flow was stopped, and H_2 was introduced at a flow rate of 56 cc/min (STP) through the by-pass loop. The 6-way valve was then switched back to the reactor mode, allowing H_2 to flow over the catalyst. The amount of CH_4 (mass 15) and C_2H_6 (mass 30)

formed initially at 303°K was monitored. The catalyst was then heated to a temperature of 973°K at a rate of 1°K/sec in flowing H_2. During this period the concentrations of CH_4 and C_2H_6 in the H_2 stream were recorded as a function of temperature.

The experimental procedures for the TPR of CO preadsorbed by the continuous-flow method and for the TPR of preadsorbed CO by the pulse method were the same except for two differences: catalyst reduction was carried out at 673°K for 2 hrs and CO adsorption was achieved by flowing pure CO over the catalyst for 1 hr at the adsorption temperature. After the adsorption of CO the gas phase CO was swept away with flowing He for 5 min, and the catalyst was cooled down to 303°K before H_2 was introduced to start a TPR experiment.

For the TPR of a flowing mixture of H_2, CO, and He, the catalyst sample was reduced and cooled to 303°K in flowing He. The reactor was then isolated from the flow system, while a gas mixture with a fixed H_2/CO ratio was prepared. The CO flow rate and total gas flow rate were always set at 19 cc/min (STP) and 285 cc/min (STP) respectively. The flow rates of H_2 and He were adjusted to give an H_2/CO ratio of 3/1 or 1/1. The gas mixture was sent through the reactor, and the concentrations of CH_4 (mass 15), together with C_2H_6 (mass 30) and C_3H_8 (mass 29), or C_2H_4 (mass 26) and C_3H_6 (mass 41) were monitored as the temperature of the catalyst sample was increased to 973°K at a rate of 1°K/sec.

In order to study the disproportionation of CO, an 8% mixture of CO in He (total flow rate = 230 cc/min (STP)) was passed over a reduced catalyst sample while its temperature was increased from 303°K to 973°K at a rate of 1°K/sec. The concentration of CO_2 was monitored as a function of temperature.

C. Catalyst Preparation

The catalyst was prepared by incipient-wetness impregnation of an alumina support (Alon C, Cabot Corp.) with a solution of $RuCl_3$. The impregnation solution was prepared by dissolving 3.288 grams of $RuCl_3 \cdot 3H_2O$ (Orion Chemical Co.) in enough distilled and deionized water to make 25 cc of saturated solution. Any excess solid was removed by filtration. An 8.2 cc volume (the volume required for incipient wetness) was mixed with 10.00 g of powdered alumina in a glass bowl and stirred until a thick black paste was obtained. The paste was spread into a thin layer over the inner surface of the bowl and frozen solid using liquid nitrogen. Th bowl was then put into a dessicator which was evacuated continously by a mechanical pump. The dessicator was immersed in a ice bath, and evacuation continued for two days. At the end of the freeze-drying period the bowl was removed from the dessicator. It was observed that the surface of the dried catalyst cake was slightly darker than the interior. This suggested that there was some nonhomogeneity in the distribution of the $RuCl_3$ in the alumina.

The dried catalyst cake was crushed and placed in a carborundum tube which was hung in a quartz tube located in a reduction furnace. The catalyst was first swept with N_2 for 30 min and then with H_2 for an additional 30 min. After that the furnace was slowly heated up to 673°K in a 1 hr period, and was held at 673°K for 2 hrs in 100 cc/min (STP) of H_2. At the end of the reduction period the catalyst was ground and sieved through a 325 Tyler mesh screen. The catalyst samples used in all experiments consisted of particles smaller than 4.5 μm.

A catalyst blank was made by following the same catalyst preparation procedures, except that distilled and deionized water was used instead of the saturated $RuCl_3$ solution.

D. Catalyst characterization

A catalyst sample and a blank sample were sent to American Spectrographic Laboratory for semi-quantitative spectrographic elemental analysis. The results shown in Table 5 indicate that the catalyst did not contain significant contaminants, and the Ru content of the catalyst was 5 wt %.

A catalyst sample was also sent to Pacific Sorption Service to determine the BET surface area and the Ru surface area by H_2 chemisorption. The BET surface area determination yielded a value of 100 m^2/g of catalyst. The adsorption of H_2 was performed at 100°C* at a H_2 partial pressure of 400 torr. The amount of H_2 adsorbed was 71 μmoles/g of catalyst. If it is assumed that one surface Ru atom chemisorbs one hydrogen atom, then the ratio of the surface Ru atoms to the total Ru atoms in the catalyst is 0.29. Using an average value of 8.17 $Å^2$ [56] for the surface area of a Ru atom and assuming that the metal particles are cubes sitting on the alumina support, the average particle size was calculated to be 50 Å.

---

*Chemisorption of H_2 is too slow at room temperature.

Table 5. Major Impurities in Ru/Al_2O_3 Catalyst and Blank (except for Ru, the reported values are wt % of the oxides of the element).

Element	Ru/Al_2O_3	Al_2O_3 (blank)
Al	95.	100
Ru	5. (as metal)	---
Fe	0.1	0.025
Ni	0.025	0.010
Si	0.025	0.004
Mg	0.008	0.006
Cr	0.006	0.004
Ca	0.006	---
Mn	0.001	0.001
Cu	0.001	---
Ti	---	---

III Results and Discussions

A. Temperature-Programmed Desorption of CO

Fig. 5 shows the TPD spectra for the desorption of CO at five different heating rates. Prior to taking each spectrum, the catalyst was saturated with CO by exposing it to 10 pulses of CO at 303°K. A He flow rate of 30 cc/min (STP) was used during desorption. Two distinct CO desorption peaks, labelled as α_1 and α_2 in Fig. 5(a), were observed for all the TPD spectra. In addition, CO_2 was formed during the desorption of CO, and two CO_2 peaks were observed. The positions of the desorption peaks shifted to lower temperature as the heating rate decreased, in agreement with the prediction of Eq. (1) and (2).

Dalla Betta [46] and Arai and Tominaga [58] have observed that CO adsorbs on alumina; therefore a blank run was performed in order to determine the effect of support adsorption on the TPD results. The spectrum for the TPD of CO from an alumina sample is shown in Fig. 6. The amount of CO desorbed from the alumina sample was less than 3% of the total amount of CO desorbed from an equal weight of Ru/Al_2O_3; therefore the adsorption of CO on the alumina support does not significantly alter the main features of the TPD spectra of CO on Ru/Al_2O_3.

In order to test whether readsorption of the adsorbate has a significant effect on the TPD results, a desorption run was performed using a He flow rate of 210 cc/min (STP). In Fig. 7 the TPD spectrum for this run is compared with a TPD run with a He flow rate of 30 cc/min (STP). A heating rate of 1°K/sec was used in both runs. The peak temperatures in Fig. 7(a) (He flow rate = 30 cc/min (STP)) are much higher than the peak temperatures in Fig. 7 (b) (He flow rate = 210 cc/min (STP)). This result clearly shows that readsorption of adsorbate does occur during the desorption

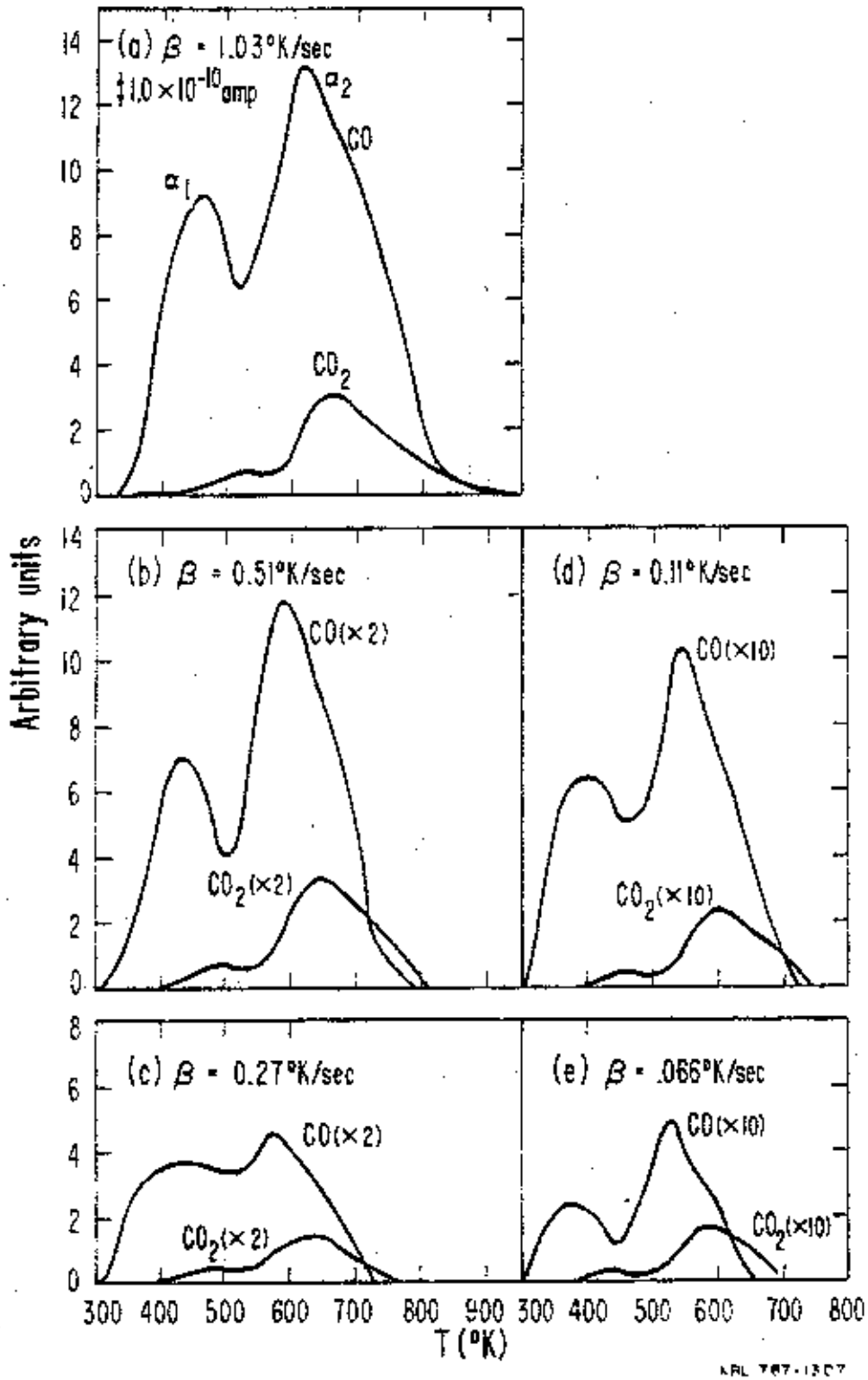

Figure 5. TPD of CO at different heating rates.

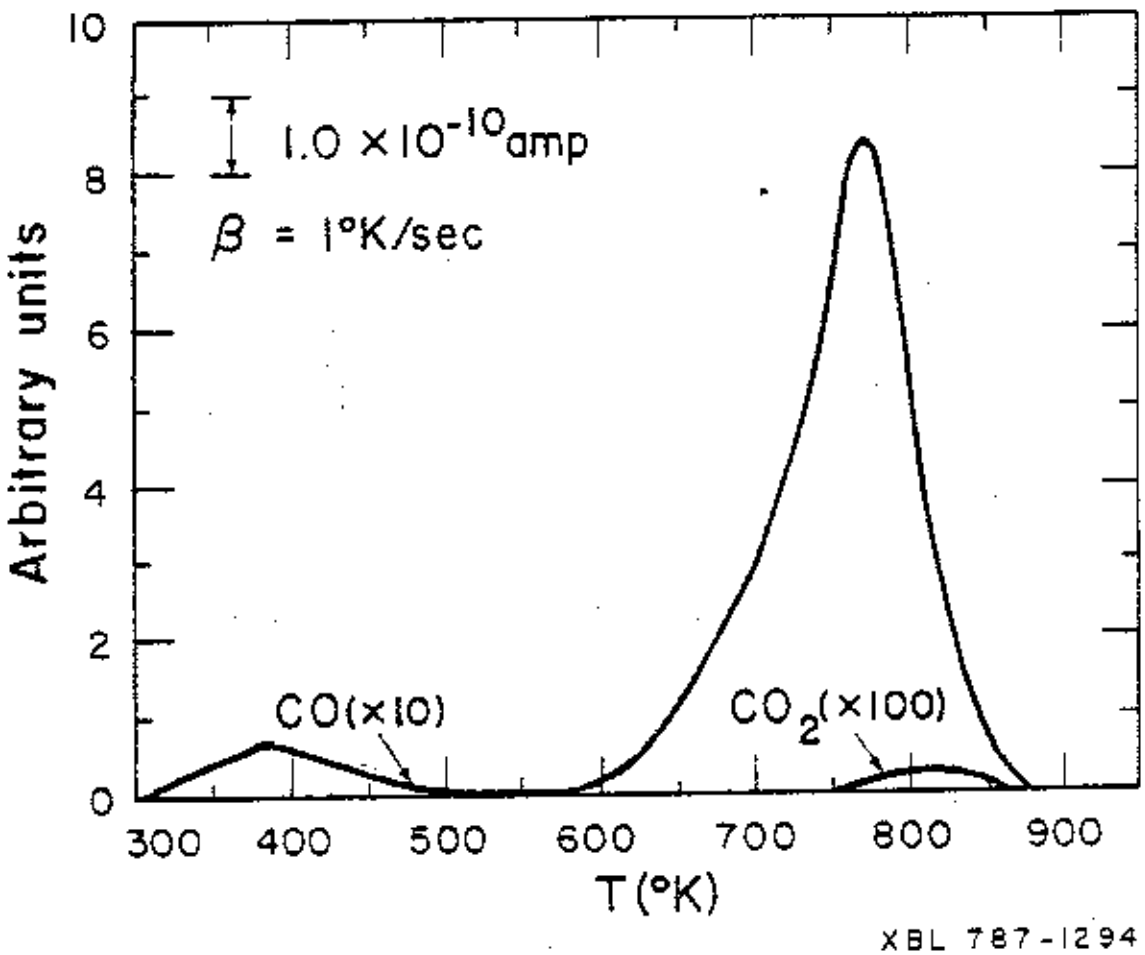

Figure 6. CO TPD from Al_2O_3 blank.

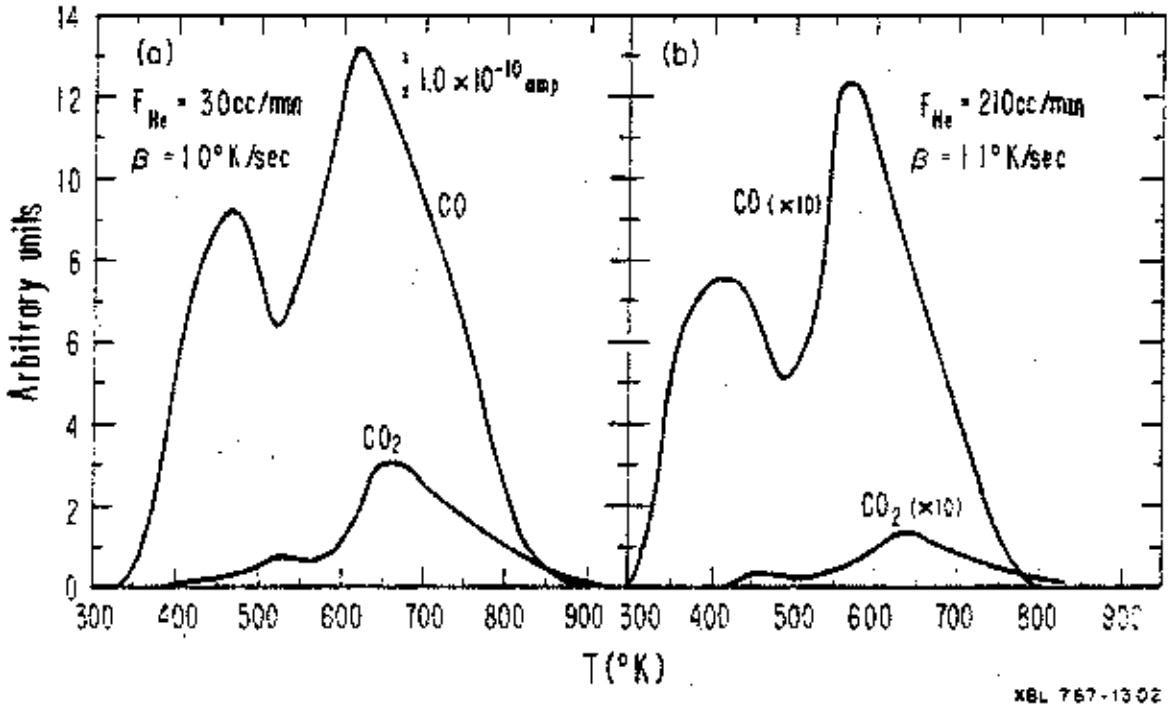

Figure 7. Effect of He flow rate on TPD of CO.

of CO at He flow rate of 30 cc/min (STP). Therefore Eq. (2), which was derived for a desorption process with freely occuring readsorption, was used to calculate the heats of desorption using the data from the TPD runs shown in Fig. 5 in which a He flow rate of 30 cc/min (STP) was used. Plots of ln T_m^2/β versus $1/T_m$ for the two CO desorption peaks are shown in Figs. 8 and 9. A least square fit was used to generate the slope of each line. The calculated values of the heat of desorption for the α_1 and α_2 peaks are 11 and 18 kcal/mole respectively.

The activation energies of desorption were calculated using Eq. (3), using a value of 10^{13} sec^{-1} for the preexponential factor. The TPD data obtained in the TPD run with a He flow rate of 210 cc/min (STP) was used in this calculation because Eq. (3) was derived for a desorption process with no readsorption. The calculated values of the activation energy of desorption are 27 and 37 kcal/mole for the two CO peaks.

The values for the activation energy agree quite well with the literature values listed in Table 4. Especially close agreement was obtained with the E_d values calculated from the TPD data of McCarty et al. [35]. Slightly higher activation energies were obtained for the TPD of CO from supported Ru than for flash desorption of CO from Ru single crystals. This is because it is impossible to completely eliminate the effect of readsorption during the desorption from a layer of powdered catalyst. Readsorption causes the desorption peaks to shift to higher temperature, resulting in an increase in the calculated values of the activation energy of desorption. The exact cause for the large difference observed between the calculated values for the activation energy and the heat of desorption is not known. It is difficult to believe that the activation energy of

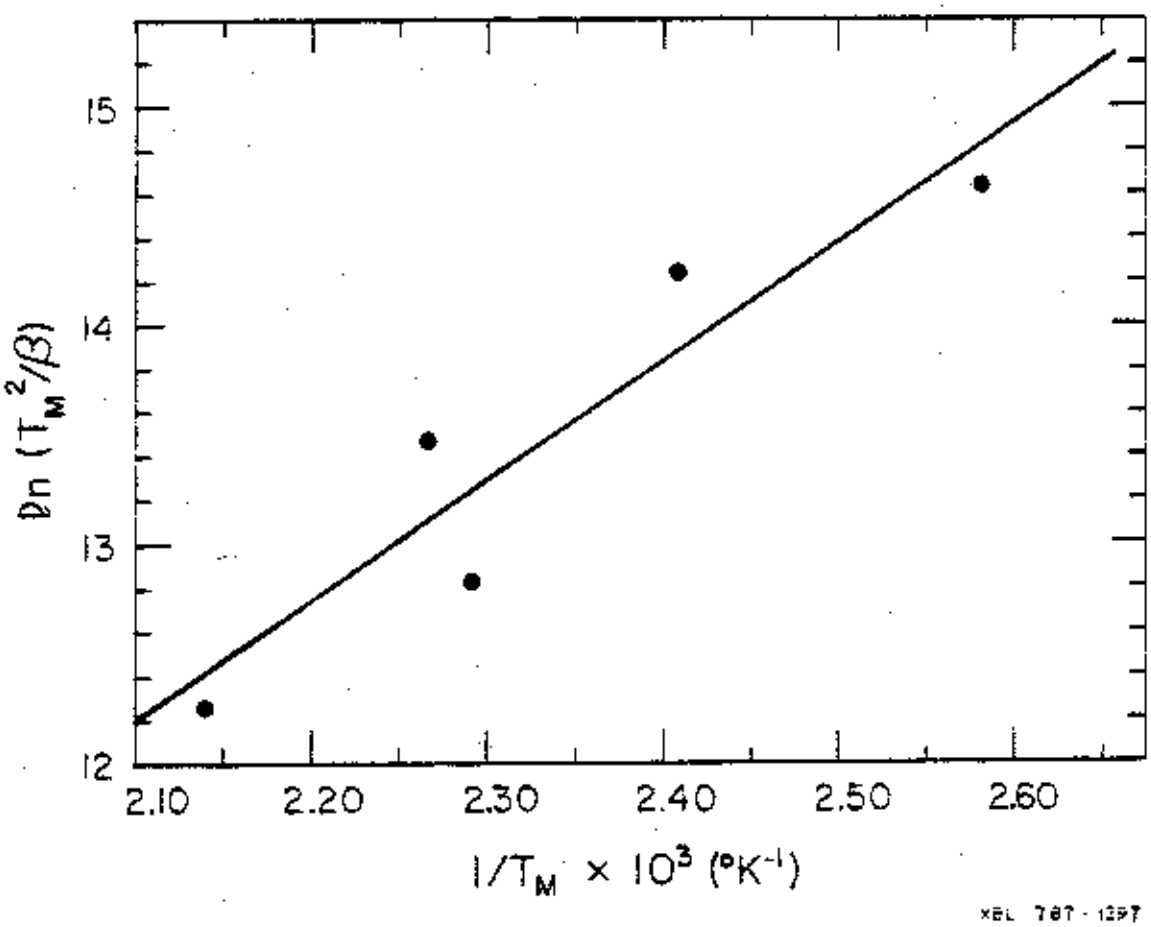

Figure 8. Heat of desorption plot for α_1 peak.

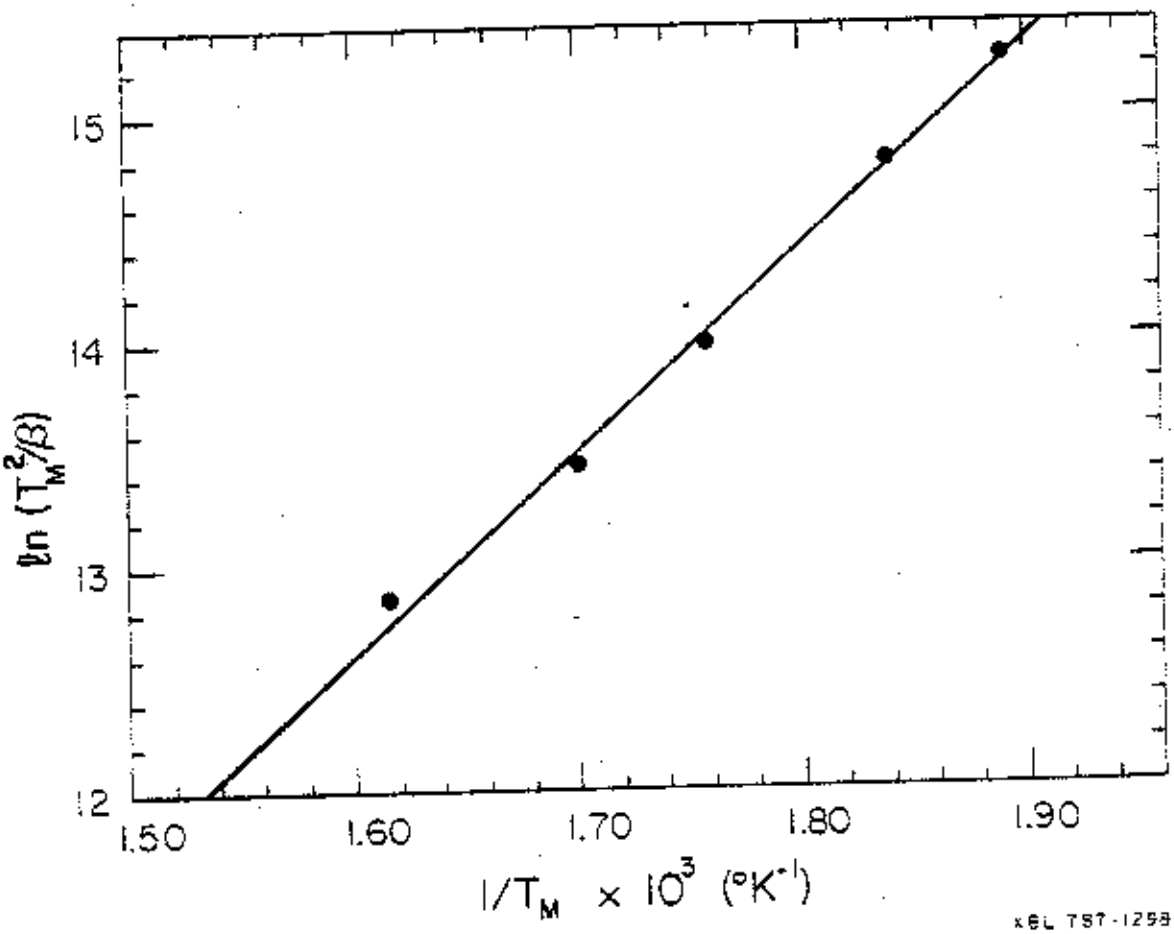

Figure 9. Heat of desorption plot for α_2 peak.

adsorption* could be as large as 19 kcal/mole for the adsorption of CO on Ru. One possible explanation is that the desorption of CO from Ru/Al_2O_3 is not a simple process. The disproportionation reaction of CO occurs as a parallel process during the desorption of CO; therefore the simple relationship between the change in peak temperature and the change in heating rate predicted by Eq. (2) was not valid.

When the present TPD results are compared with those in the literature, good agreement is obtained (see Table 4). Flash desorption studies of CO on Ru(001), (101), and (100) surfaces [52-55] showed two CO desorption peaks having desorption temperatures corresponding to the desorption temperatures of the α_1 and α_2 peaks observed in this study. However only one CO desorption peak was observed on Ru(110) [42]. CO_2 was never observed during the flash desorption of CO from Ru single crystals under vacuum conditions. A TPD study by McCarty et al. [35] found three CO desorption peaks for Ru/Al_2O_3, and they observed CO_2 formation during the TPD of CO. The low and intermediate temperature CO peaks in their study corresponded to our α_1 and α_2 peak, respectively, but their high temperature CO peak was not clearly observed in our study, although the slight broadening at the high temperature shoulder of the α_2 peak observed in the spectra shown in Figs. 5 and 7 can be attributed to the existence of a poorly resolved high temperature peak.

Based on the evidence from LEED and XPS [42, 52-55] studies, it is generally agreed that the two desorption peaks observed in the flash

---

* The activation energy of adsorption is equal to the difference between the activation energy of desorption and the heat of desorption.

desorption studies are due to the desorption of molecularly adsorbed CO. Therefore the α_1 and α_2 peaks observed in this study are probably due to the desorption of molecular CO from the Ru surface. However it is still unclear whether the two peaks arise from the desorption of CO from two distinct adsorption sites or are merely due to CO-CO repulsive interactions. Madey and Menzel [52] suggested that the two adsorbed states of CO observed on Ru (001) are due to CO-CO repulsive interactions, but Reed et al. [54] argued that the two adsorbed states of CO observed on Ru(101) are due to adsorption on different sites. There has been no evidence which suggests the existence of a third CO peak in all the flash desorption study of CO on Ru single crystals under vacuum conditions. The nature of the high temperature CO peak which was observed by McCarty et al. [35] and in this study will be discussed in greater detail later.

In this study and the study by McCarty et al. [35], CO_2 was always formed during the TPD of CO. The disproportionation reaction of CO was studied further in a continuous flow TPR run. A gas mixture in which the CO/He ratio was 0.09 was passed over the catalyst while the temperature of the reactor was increased from 303°K to 973°K at 1°K/sec. The concentration of CO_2 in the gas stream was monitored. The result is shown in Fig. 10. CO_2 began to appear at 415°K and the concentration reached a maximum at approximately 700°K. The decline in CO_2 concentration at high temperature was probably due to the saturation of the Ru surface by carbon, a product of the disproportionation reaction.

As mentioned earlier CO_2 was not observed during the flash desorption of CO from Ru single crystals under vacuum conditions, and attempts to

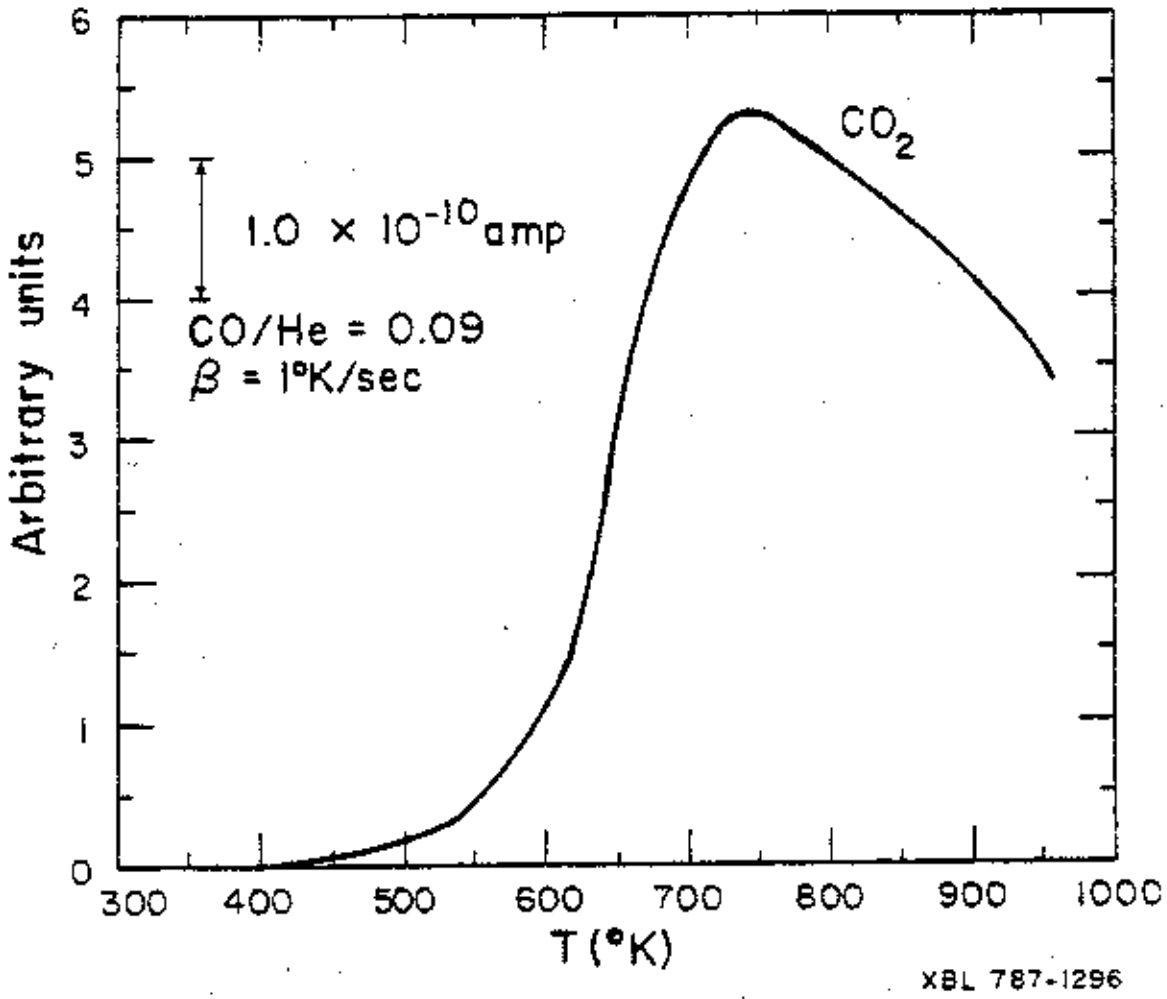

Figure 10. Disproportionation of CO in continuous flow TPR.

thermally induce the disproportionation of CO on Ru single crystals in low partial pressure of CO have been unsuccessful. Heating a Ru(110) crystal in 10^{-3}torr of CO at 630°K for 30 min [42] and heating a Ru(101) crystal in 10^{-7}torr of CO to 1073°K [54] had failed to disproportionate CO. However when a layer of adsorbed CO was bombarded by the electron beam from a LEED gun, desorption and dissociation of CO were observed [52-54]. Subsequent flash desorption of the bombarded CO adlayer resulted in the appearance of a new desorption peak with a peak temperature in the range of 550-600 K [53]. XPS evidence showed that the new state was dissociated CO occupying two surface sites.

One must now address the question of why was CO_2 formed during the TPD of a CO from Ru/Al_2O_3 in a flow system but not during the flash desorption of CO from Ru single crystals in a vacuum system. The formation of CO_2 is clearly not a support effect since Singh and Grenga [59] have observed that by exposing a polycrystalline Ru sphere to 760 torr of CO at 823°K, carbon was deposited on the Ru surface. This suggests that the partial pressure of CO over the catalyst is an important factor in determining whether CO disproportionation takes place or not. An Eley-Rideal mechanism for CO disproportionation is proposed here in order to explain the pressure dependency of the reaction.

$$CO_{(s)} \rightleftharpoons C_{(s)} + O_{(s)} \qquad \text{(slow step)}$$

$$CO_{(g)} + O_{(s)} \longrightarrow CO_{2(g)}$$

The equilibrium for the dissociations of CO is not favorable, but the removal of surface oxygen by gas phase CO shifts the dissociation reaction to the right. If the concentration of CO in the gas phase is very low, which is true during the flash desorption of CO in a fast

pumping vacuum system, CO_2 formation cannot occur. Also the concentration of dissociated CO must be very small on the catalyst surface because even under a significant partial pressure of CO (10^{-3} torr), disproportionation does not occur on a Ru (110) crystal kept at 630°K. Other evidence which supports the Eley-Rideal mechanism can be seen by comparing the relative amount of CO_2 formed for the TPD runs with 210 cc/min (STP) of He and 30 cc/min (STP) of He. The ratio of the amount of CO_2 formed to the amount of CO desorbed is 0.08 for the run with 210 cc/min (STP) of He and is 0.15 for the run with 30 cc/min (STP) of He. Relatively less CO_2 was formed for the run with the higher the flow rate because the concentration of CO in the gas phase is lower during this run.

Carbon, accumulated on the catalyst surface during desorption, can enhance the strength of adsorption of CO by donating electrons to increase the degree of back bonding between the carbon atom of an adsorbed CO molecule and the Ru surface atoms [60]. An increase in the degree of back bonding weakens the C-O bond but strengthens the C-Ru bond. This phenomenon was observed by Dalla Betta [40] in the infrared study of CO on Ru/Al_2O_3. He observed that the presence of carbon on the Ru surface lowered the stretching frequency of the adsorbed CO. This trend implied a weakening of the C-O bonds and a strengthening of the C-Ru bonds. The strengthening of the C-Ru bonds of the adsorbed CO could explain the fact that a high temperature peak was observed during the desorption of CO from Ru/Al_2O_3 but not from Ru single crystals (Carbon was not formed during the flash desorption of CO from Ru single crystals.).

A series of runs which shows the effect of adsorption temperature on the TPD of CO is shown in Fig. 11. The catalyst sample was first

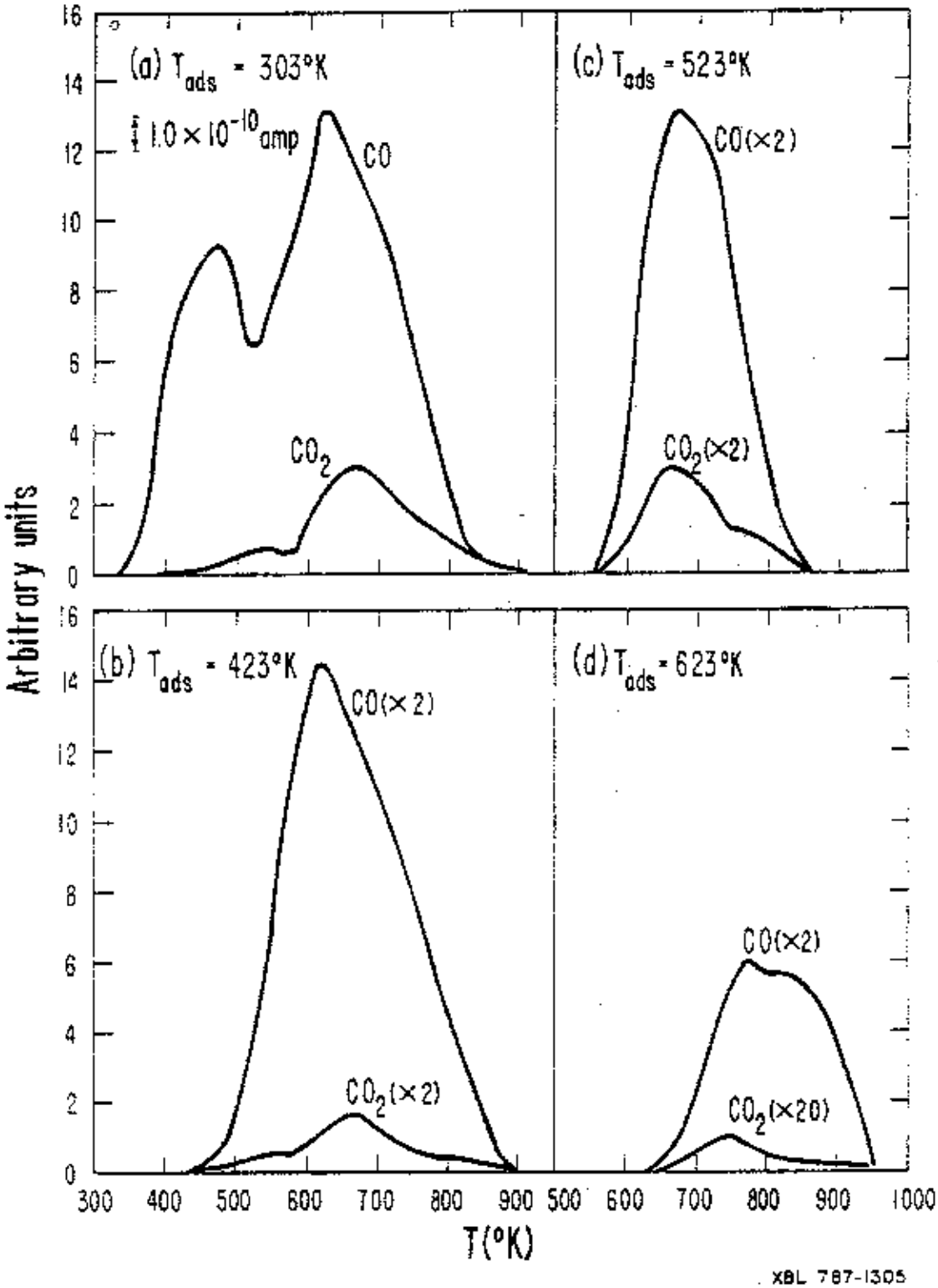

Figure 11. TPD of CO adsorbed at different temperature by pulse adsorption.

exposed to 10 pulses of CO at the adsorption temperature and then cooled down to 303°K in flowing He. A desorption spectrum was taken while the temperature was increased to 973°K at 1°K/sec. CO_2 was formed during the adsorption of CO at an adsorption temperature of 423°K or greater, and the amount of CO_2 trapped in the liquid nitrogen trap increased with increasing adsorption temperature. The results of these experiments showed that it is possible to preferentially adsorb only the strongly bound CO by adsorbing at high temperature. The enhancement of the adsorption strength of CO by surface carbon can be seen in Fig. 11(d). Here the desorption of CO occurred at very high temperature.

B. Temperature-Programmed Reaction of CO in Flowing H_2

The reactivity of the CO adsorbed at different temperatures was examined in the TPR runs shown in Fig. 12. The catalyst was first exposed to 10 pulses of CO at the adsorption temperature and then cooled down th 303°K in flowing He. The CO_2 formed during the adsorption was trapped with the liquid nitrogen trap and quantitatively analyzed using the mass spectrometer. After the adsorption of CO, He flow was stopped and H_2 was passed over the catalyst. The amount of CH_4 formed at 303°K was monitored, and then the catalyst was heated up in flowing H_2 at a rate of 1°K/sec while the concentrations of CH_4 and C_2H_6 in the H_2 stream were recorded.

No CO_2 was detected during the adsorption of CO at 303°K and only a small amount of CO_2 was detected at 423°K. The CO adsorbed at 303°K and 423°K did not react with H_2 at 303°K. CH_4 formation did not begin until the reactor was heated up. The rate of CH_4 formation reached a maximum at 460°K. But when carbon was deposited on the catalyst by

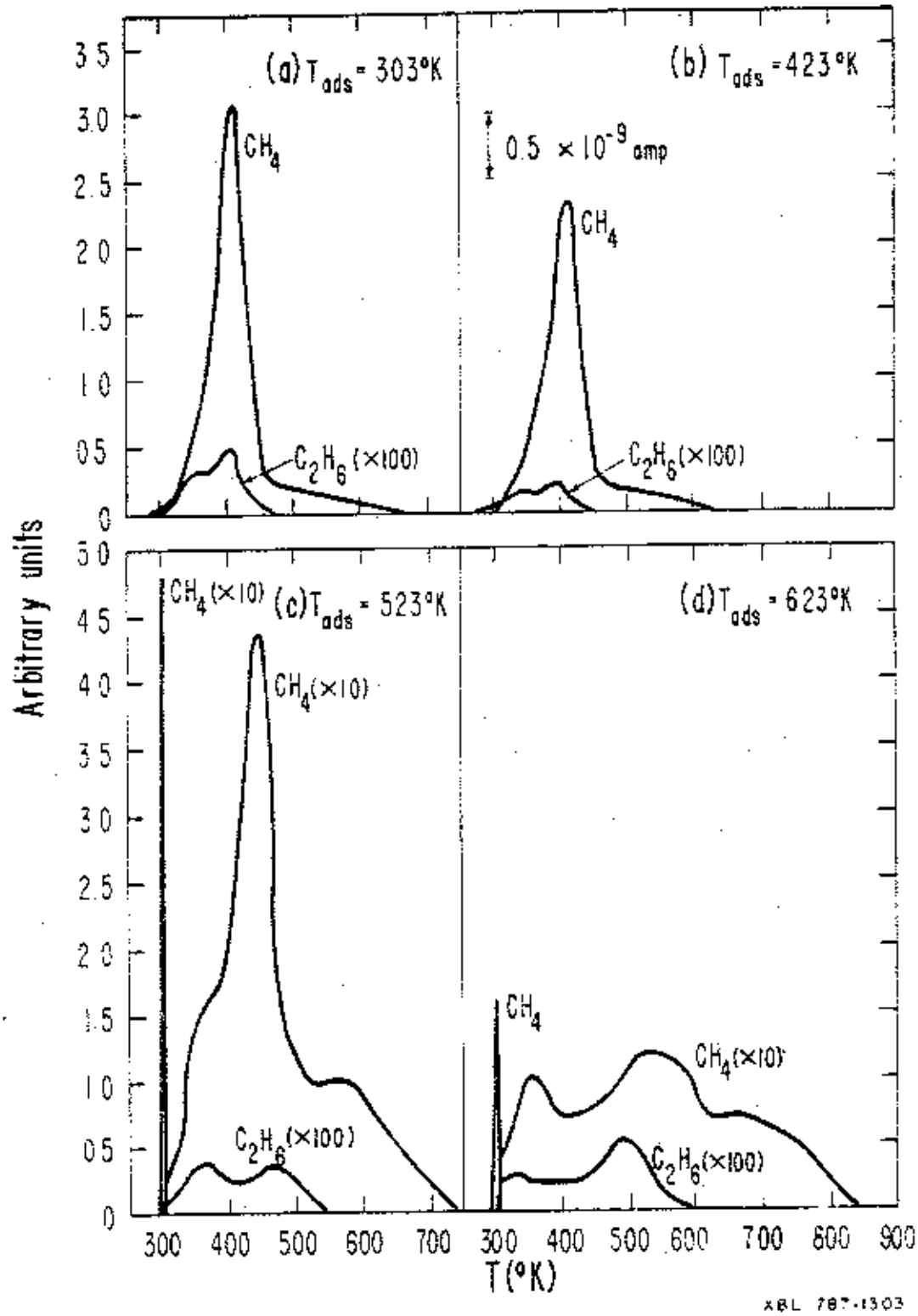

Figure 12. TPR of CO adsorbed at different temperature by pulse adsorption.

adsorbing CO at 523 and 623°K, as indicated by the appearance of CO_2 during adsorption, a large amount of CH_4 was formed when H_2 was introduced at 303°K. A small amount of C_2H_6 was also detected. The narrow spikes in Figs. 12(c) and 12(d) represent the rate of CH_4 formation at 303°K. In Fig. 12(d) the initial rate of CH_4 formation at 303°K is an order of magnitude greater than the maximum rate of CH_4 formation during the TPR run.

Table 6 summarizes the TPR results quantitatively. The quantities listed in Table 5 are in units of uncalibrated area obtained by integrating the TPR spectrum (The sensitivity of the mass spectrometer is different for different masses, and this was not accounted for in Table 6.). The greater the amount of carbon deposited during CO adsorption, the greater the amount of CH_4 was produced at 303°K. These results strongly suggest that carbon was the reactive species responsible for the formation of CH_4 at 303°K. One would expect that the amount of carbon deposited (or the amount of CO_2 formed during adsorption) to be equal to the amount of CH_4 formed at 303°K. However such a mass balance was not observed as shown in the last column of Table 6. Even though the areas are uncalibrated and therefore the ratio of CH_4(@303°K)/CO_2 has no direct physical significance, one should expect that this ratio to be constant at different adsorption temperatures if the mass balance between carbon (or CO_2) and CH_4(@303°K) holds. This discrepancy is due to the fact that thermal aging of the carbon deposit leads to a loss in its reactivity. Thermal treatment converts the reactive form of carbon (carbidic carbon) to an unreactive form of carbon (graphitic carbon). The graphitic carbon is even less reactive in H_2 than molecular CO, and a very high temperature is required to hydrogenate it to form CH_4. The hydrogenation of this graphitic carbon

Table 6. Results on the TPR of CO *

Adsorption temperature (°K)	CO_2 (formed during adsorption)	CH_4(@303°K)	Total CH_4 formed	CH_4(@303°K)/CO**
303	0	0	0.178	--
423	0.0005	0	0.146	--
523	0.0026	0.0050	0.0481	1.94
623	0.0164	0.0075	0.0358	0.46

* The amounts are expressed in units of uncalibrated area. The difference in sensitivity of the mass spectrometer for different masses has not been accounted for.

** The ratio of two uncalibrated area has no physical significance. The comparison is made to see whether the ratio is constant or not at different adsorption temperatures.

leads to the appearance of a high temperature CH_4 peak, which can be seen at 570°K in Fig. 12 (c) and at 660°K in Fig. 12(d). Similar deactivation of the reactive carbon at high temperature has been reported on Ni [24].

A low temperature CH_4 peak can also be seen in Figs. 12(c) and 12(d) at approximately 350°K. As discussed in the previous section the presence of surface carbon weakens the C-O bond of the adsorbed CO by donating electrons to enhance the back bonding between the metal and the carbon atom of the adsorbed CO. Therefore the "weakened" CO can dissociate at a lower temperature to react with H_2 to form CH_4, which explains the appearance of the low temperature CH_4 peak at approximately 350°K in Figs. 12(c) and 12(d).

The effect of thermal aging on the reactivity of the carbon deposit was further examined in the series of runs shown in Fig. 13. The catalyst was exposed to flowing CO at 760 torr for 1 hr at the adsorption temperature. The excess CO was then swept away with He, and H_2 was introduced to begin the TPR run, the TPR spectra in Fig. 13(a) to 13(d) are similar to the ones shown in Fig. 12. Only one CH_4 peak was observed for the runs with adsorption temperature at 303°K and 373°K, but three CH_4 peaks were observed for the runs with adsorption temperature at 473°K and 573°K. The highest temperature CH_4 peak first appeared as a tail on the major CH_4 peak in Figs. 13(a) and 13(b), and it grew into a major peak in Figs. 13(c) and 13(d). In fact, for the run with an adsorption temperature of 623°K, the highest temperature CH_4 peak became the only peak as shown in Fig. 13(e). The aged carbon was so unreactive that in Fig. 13(e) the rate of CH_4 formation did not reach a maximum until the temperature was 890°K.

The effect of temperature and H_2/CO ratio on the rate of methanation and product distribution was investigated in a series of continuous flow TPR runs. A CO-H_2 mixture diluted in He was passed over the catalyst

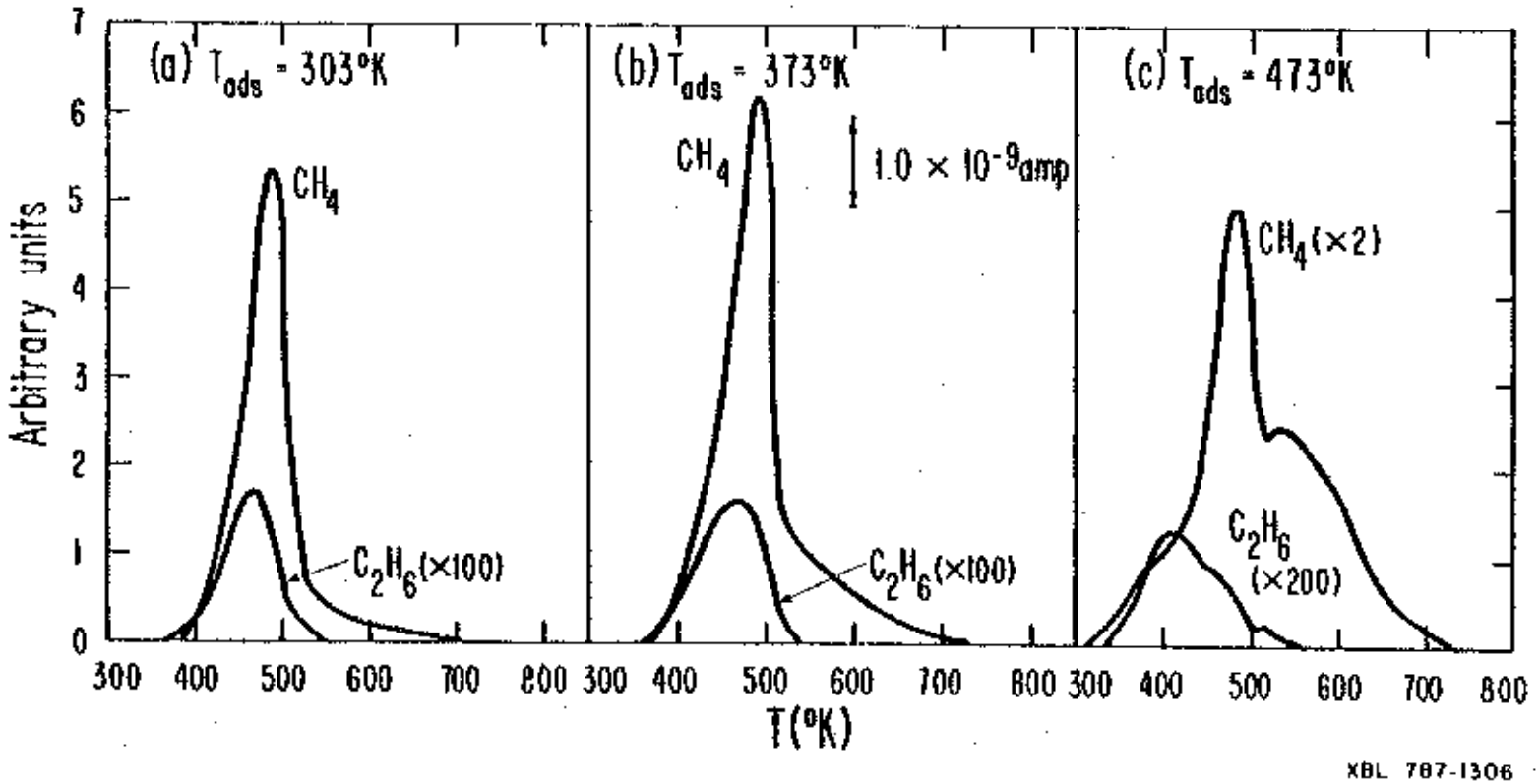

Figure 13. TPR of CO adsorbed at different temperature by continuous flow adsorption for 1 hr.

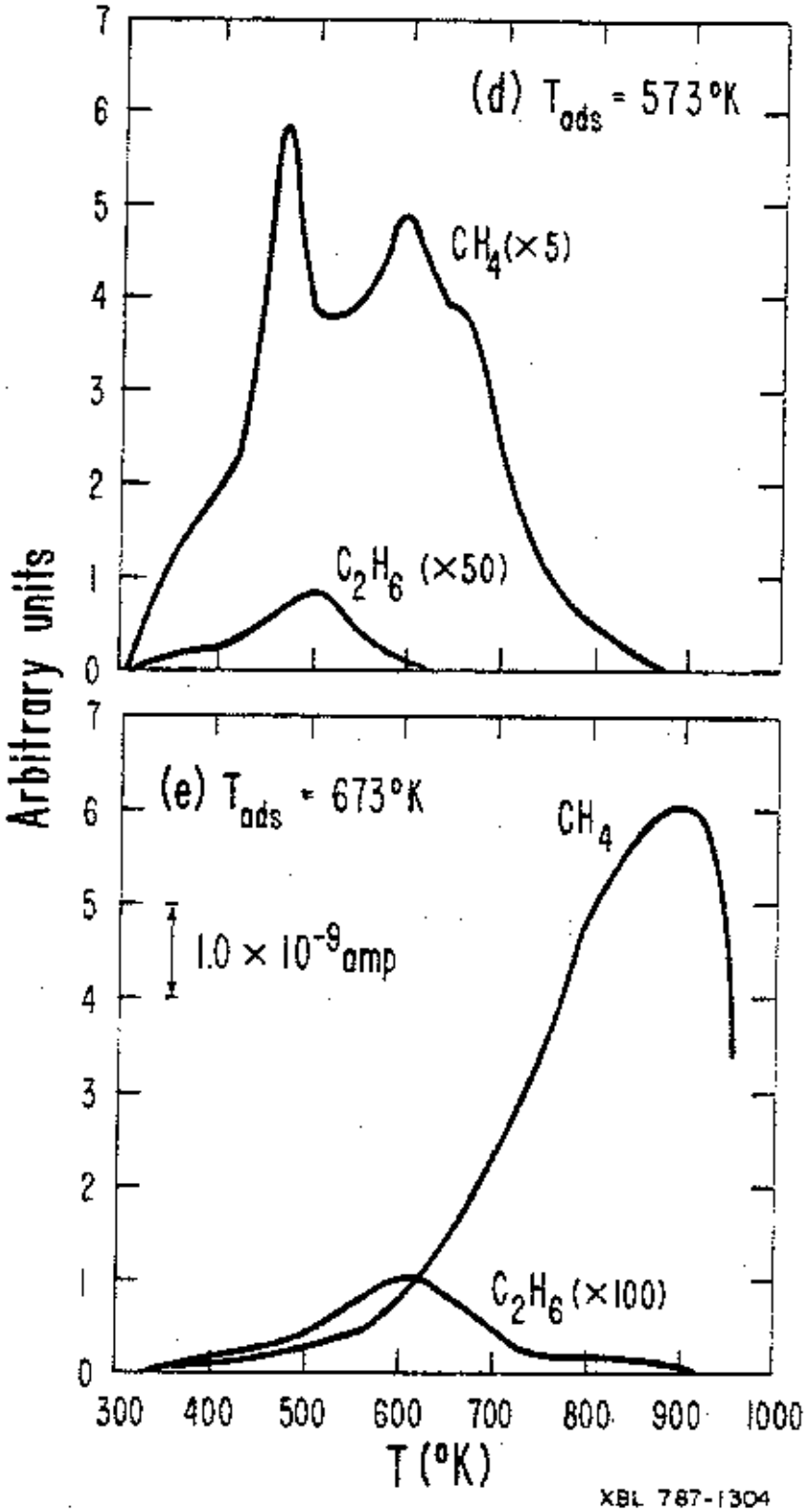

Figure 13. (Continued).

while the temperature of the reactor was increased at a rate of 1°K/sec The concentrations of CH_4, C_2H_6, and C_3H_8 or the concentration of CH_4, C_2H_4, and C_3H_6 were monitored as a function of temperature. The results are shown in Figs. 14 to 17.

CH_4 was the predominant product for all the run. Only a small amount of C_2 products were detected, and no C_3 product was detected at all. Low reaction temperature favored the formation of C_2 products over the formation of CH_4, but the opposite was true at high reaction temperature. The rate of CH_4 formation decreased by three orders of magnitude when the ratio of H_2/CO was changed from 3 to 1. The drop in the rate of of CH_4 formation at very high temperature was due to thermodynamics limitation because the methanation rate increased when the reactor was cooled down. For the runs with H_2/CO ratio of 2.8 and 3.0, the large amount of heat released during the formation of CH_4 affected the linearity of the temperature ramp. For the runs with H_2/CO ratio of 1.0, a change in the rate of CH_4 production was observed near 650°K. This observed change in the methanation rate can be explained by the following discussion. At a H_2/CO ratio of 1.0, the conditions of the reaction are such that the formation of carbon by disproportionation of CO is favored. Because the partial pressure of H_2 is low, the rate of carbon removal by formation of CH_4 is lower than the rate of carbon formation. A decrease in the methanation rate is observed when the catalyst surface is covered with an unreactive carbon layer. However, at a sufficiently high temperature, the methanation rate picks up again because the unreactive carbon can be hydrogenated, and the catalyst surface is regenerated for the reaction to take place once again.

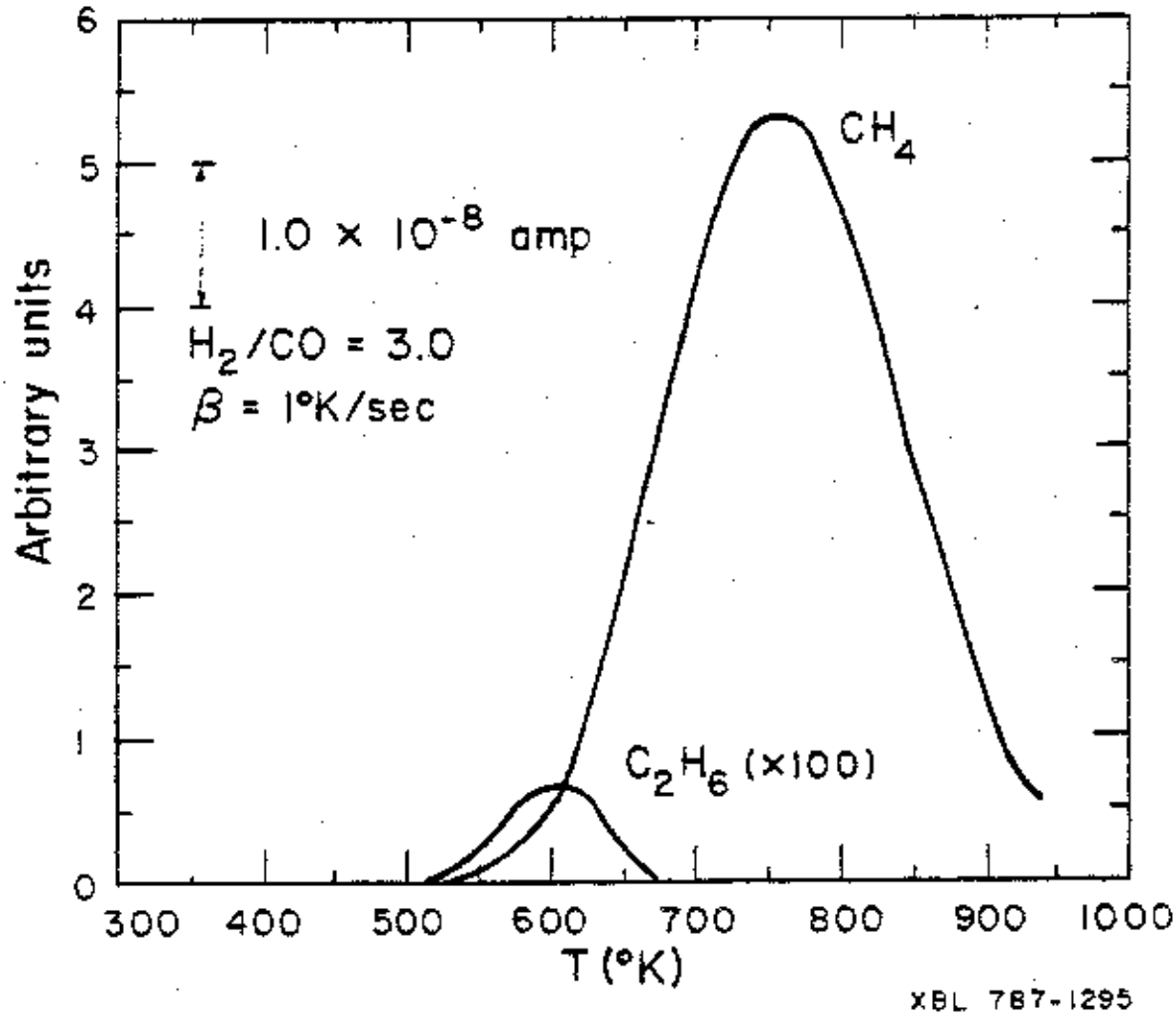

Figure 14. Continuous flow TPR of $CO-H_2$ mixture.

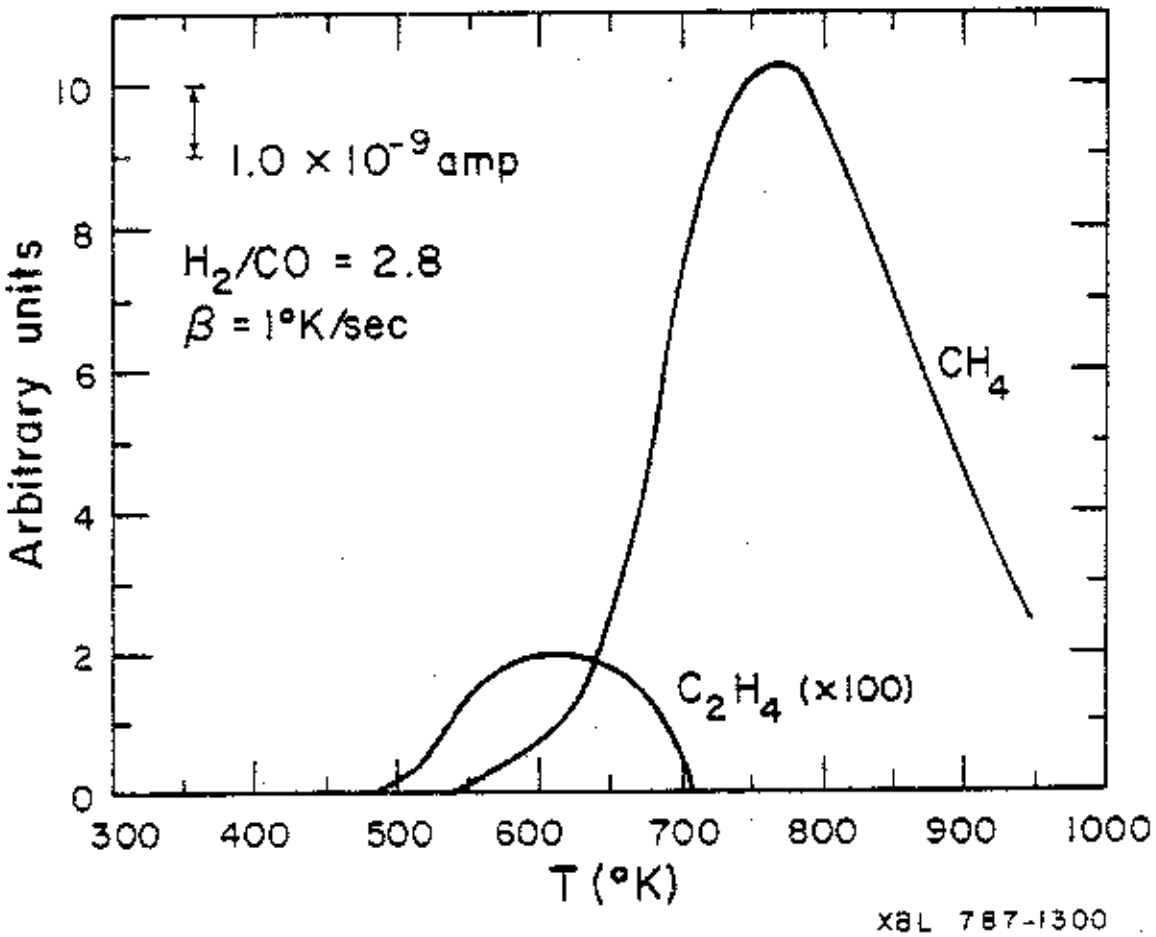

Figure 15. Continuous flow TPR of $CO-H_2$ mixture.

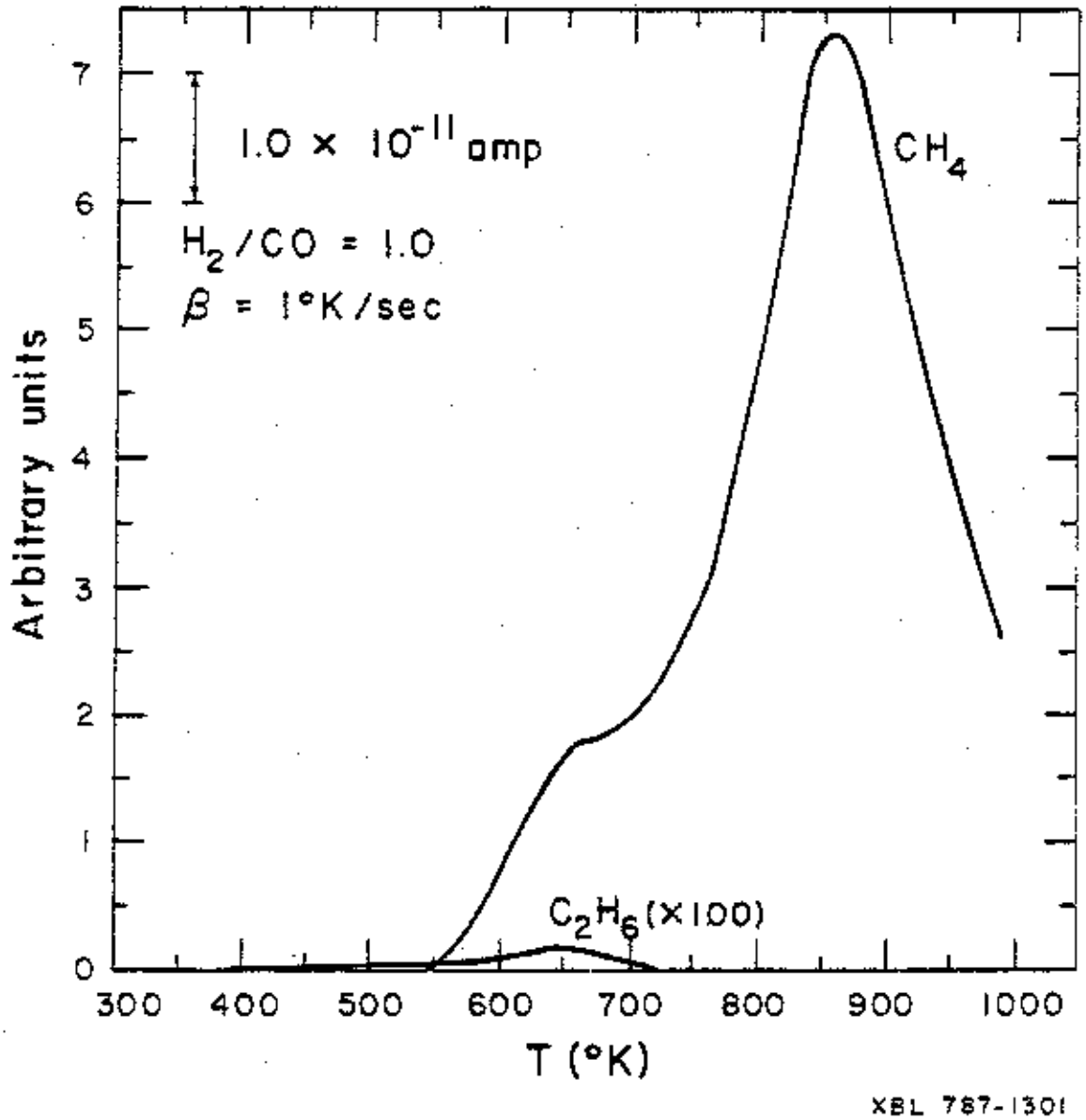

Figure 16. Continuous flow TPR of CO-H_2 mixture.

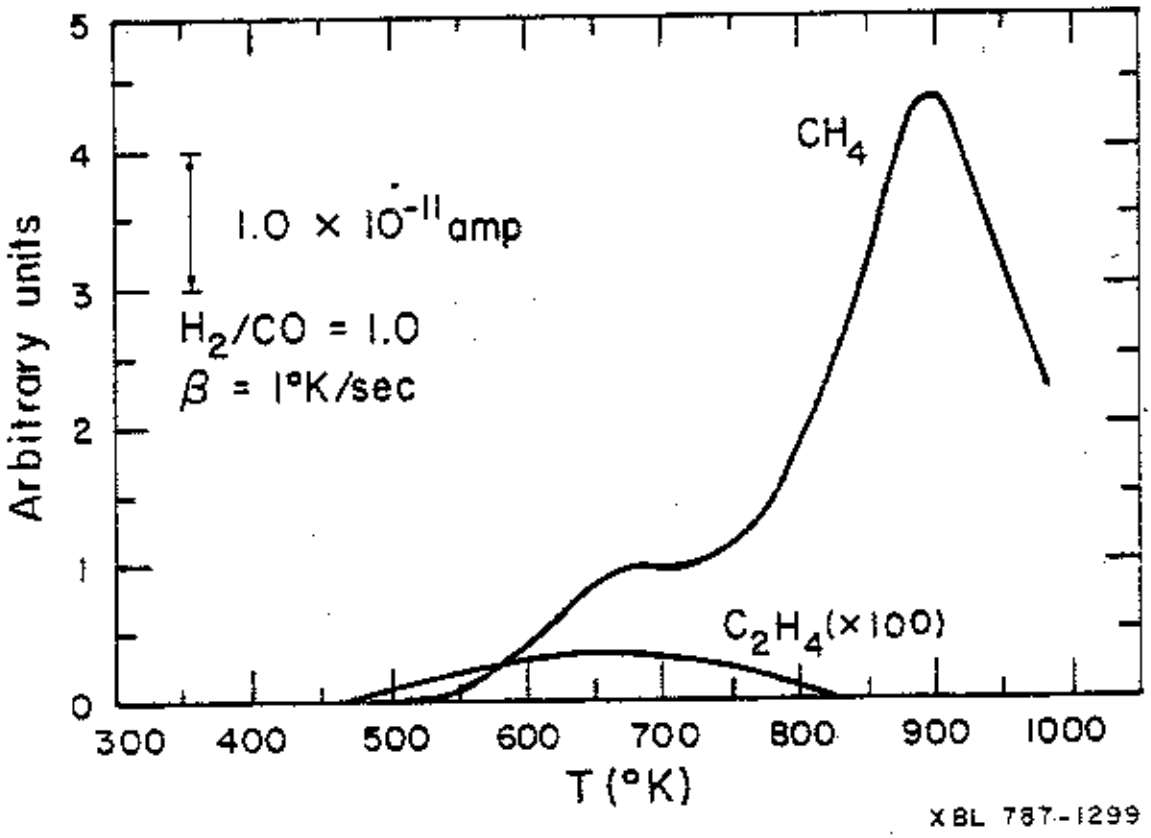

Figure 17. Continuous flow TPR of $CO-H_2$ mixture.

IV. Conclusions

CO adsorbs molecularly on Ru/Al_2O_3 at 303°K in two different states. TPD of CO from Ru/Al_2O_3 gives rise to two distinct CO peaks with activation energies of desorption of 27 and 37 kcal/mole. CO_2 was observed during the TPD of CO from Ru/Al_2O_3, but CO_2 formation was not observed during the flash desorption of CO from Ru single crystals. This observation was explained by postulating an Eley-Rideal mechanism for CO_2 formation in which gas phase CO reacts with the adsorbed oxygen derived from the dissociation of CO to form CO_2. Carbon left on the catalyst surface by the disproportionation reaction can enhance the strength of adsorption of CO by providing electrons to increase the degree of back bonding between the carbon of the adsorbed CO and the metal atoms.

The results of the TPR experiments are in general agreement with the carbide theory proposed for the reaction of CO and H_2 to form methane and hydrocarbons. A reactive carbon can be deposited on the Ru/Al_2O_3 catalyst by the disproportionation of CO at high temperature ($T \geq 415°K$). This carbon can react readily with H_2 at 303°K to produce CH_4 and small amounts of C_2H_6, but adsorbed CO was inert to H_2 at this temperature. The reactive carbon can be easily converted into an unreactive carbon by thermal treatment. This unreactive carbon is even less reactive toward H_2 than CO. These results strongly suggest that carbon is the reactive intermediate in the methanation reaction. The rate determining step in the formation of CH_4 is the dissociation of CO on the catalyst surface. In the presence of H_2 the dissociated CO reacts rapidly to form CH_4 and H_2O. The mechanism of CO disproportionation is similar to the mechanism of CH_4 formation. The dissociation of CO is also the rate determining

step in the disproportionation of CO. Once dissociated CO is formed on the catalyst surface, the CO in the gas phase reacts with the surface oxygen to form CO_2, leaving carbon on the catalyst surface.

The mechanism of chain growth in the formation of higher molecular hydrocarbons cannot be deduced from the results of this study. The fact that a small amount C_2H_6 was formed when the carbon-covered catalyst was exposed to H_2 at 303°K seems to indicate that a possible mechanism for chain growth is the polymerization of the CH_2 units, but further studies are needed before a plausible mechanism can be proposed.

Acknowledgments

The advice and guidance given by Professor Alexis T. Bell is greatly appreciated and a special thanks goes to Dr. Henry Wise and Mr. John G. Ekerdt for their helpful discussions and assistances.

This work was done under the auspices of the U.S. Department of Energy.

V. References

[1] D.A. King, Surface Sci. 47, 384 (1975).

[2] R.J. Cvetanović and Y. Amenomiya, Catal. Rev. 6(1), 21 (1972).

[3] M. Smutek, S. Černý, and F. Buzek, Advan. Catal. 24, 34 (1975).

[4] D. Menzel, in "Topics in Applied Physics", Vol. 4 (R. Gomer, ed.) Spring-Verlag, New York, (1975) Chap. 4.

[5] R.J. Cvetanović and Y. Amenomiya, Advan. Catal. 17, 103 (1967).

[6] Y. Amenomiya and R.J. Cvetanović, Phys. Chem. 67, 144 (1963).

[7] P.A. Redhead, Vacuum 12, 203 (1962).

[8] F.M. Lord and J.S. Kittleburger, Surface Sci. 43 173 (1974).

[9] M. Greyson, in "Catalysis", Vol. 4 (P.H. Emmett, ed.) Reinhold, New York, (1956) Chap. 6.

[10] R.B. Anderson, Ibid., Chaps. 1,2,3, and 4.

[11] G.A. Mill, and F.W. Steffgen, Catal. Rev. 8(2), 159 (1973).

[12] H. Pichler, Advan. Catal. 4, 271 (1952).

[13] H. Pichler and A. Hector, Kirk-Othmer Encyclopedia Chem. Tech. IV, 446 (1964).

[14] H. Pichler and H. Schulz, Chem. Ing. Tech. 42, 162 (1970).

[15] B.K. Nefedov and Y.T. Eidus, Russ. Chem. Rev. 34, 272 (1965).

[16] H. Storch, N. Golumbic, and R. Anderson, "The Fischer-Tropsch and Related Synthesis", Wiley, New York, (1951).

[17] M.A. Vannice, Catal. Rev.-Sci. Eng., 14(2), 153 (1976).

[18] G. Natta, in "Catalysis" Vol. 3 (P.H. Emmett, ed.) Reinhold, New York, (1955) Chap. 8.

[19] F. Fischer and H. Tropsch, Brennst.-Chem. 7, 97 (1926).

[20] J.A. Rabo, A.P. Risch, and M.L. Poustma, "The Mechanisms of Hydrocarbon Synthesis from CO + H_2 over Group VIII Metal Catalysts" to be published.

[21] J.T. Kummer and P.H. Emmett, J. Amer. Chem. Soc. 75, 5177 (1953).

[22] W.K. Hall, R.J. Kokes, and P.H. Emmett, Ibid., 82, 1027 (1960).

[23] J.T. Kummer, T.W. DeWitt, and P.H. Emmett, J. Amer. Chem. Soc. 70, 3632 (1948).

[24] S. Weller, J. Amer. Chem. Soc. 69, 2432 (1947).

[25] S. Weller, L.J.E. Hofer, and R.B. Anderson, J. Amer. Chem. Soc. 70, 799 (1948).

[26] Y.T. Eidus, and N.D. Zelinskii, Izv. Akad. Nauk. SSSR, Otd. Khim. Nauk, 45 (1942), 190 (1942).

[27] Y.T. Eidus, Izv. Akad. Nauk SSSR. Otd. Khim. Nauk, 447 (1946).

[28] Y.T. Eidus, Bull. Acad. Sci. URSS Classe Sci. Chim. 41, 190 (1942), 44, 255 (1944).

[29] C.C. Hall and S.L. Smith, J. Soc. Chem. Ind. London 65, 128 (1946).

[30] K.A. Kini and A. Lahiri, J. Sci. Ind. Res., 34, 97 (1975).

[31] G. Bhyholder and L.D. Neff, J. Phys. Chem. 66, 1664 (1962).

[32] V.M. Vlasenko and G.E. Yuzefovich, Russ. Chem. Rev. 38(9) 728 (1969).

[33] H. Matsumoto and C.D. Bennett, "Methanation and Fischer-Tropsch Reactions over Fused Iron Catalyst", to be published.

[34] P.R. Wentrek, B.J. Wood, and H. Wise, J. Catal. 43, 363 (1976).

[35] J. McCarty, P. Wentrek, and H. Wise, "Carbon Formation on Alumina-supported Ruthenium Catalyst" to be published.

[36] M. Araki and V. Ponec , J. Catal. 44 439 (1976).

[37] M.A. Vannice, J. Catal. 37 449 (1975).

[38] R.A. Dalla Betta, A.G. Piken, and M. Shelef, J. Catal. 35, 54 (1974).

[39] Ibid., 40, 173 (1975).

[40] R.A. Dalla Betta and M. Shelef, J. Catal. 48, 111 (1977).

[41] K. Kraemer and D. Menzel, Ber. Bunsenges Phys. Chem. 79, 649 (1975).

[42] D.W. Goodman, T.E. Madley, M. Ono, and J.T. Yates Jr., J. Catal. 50, 279 (1977).

[43] R.R. Ford, "Advan. Catal." 21, 51 (1970).

[44] J.H. Sinfelt and D.J.C. Yates, J. Catal. 8, 82 (1967).

[45] N.E. Buyanova, A.P. Karnaukhov, N.G. Koroleva, I.D. Ratner, and O.N. Chernyavaskaya, Kinitika i Kataliz 13(6), 1533 (1972).

[46] R.A. Dalla Betta, J. Phys. Chem. 79, 2519 (1975).

[47] L. Lynds, Spectrochem. Acta. 20 1369 (1964).

[48] C.R. Guerra and J.H. Schulman, Surface Sci. 7, 229 (1967).

[49] M. Kobayashi and T. Shirasaki, J. Catal. 8, 289 (1973).

[50] M.F. Brown and R.D. Gonzalez, J. Phys. Chem. 80, 1731 (1976).

[51] A.A. Davydov and A.T. Bell, J. Catal. 49, 332 (1977).

[52] T.E. Madey, and D. Menzel, Japan J. Appl. Phys. Suppl. 2, Pt. 2, 229 (1974).

[53] J.C. Fuggle, E. Umbach, P. Feulner, and D. Menzel, Surface Sci. 64 69 (1977).

[54] P.D. Reed, C.M. Comrie, and R.M. Lambert, Surface Sci. 59 33 (1976).

[55] R. Ku, N.A. Gjostein, and H.P. Bonzel, Surface Sci. 64, 465 (1977).

[56] R.A. Dalla Betta, J. Catal. 34, 57 (1974).

[57] K.C. Taylor, J. Catal. 38 299 (1975).

[58] H. Arai and H. Tominaga J. Catal. 43, 131 (1976).

[59] K.J. Singh and H.E. Grengra J. Catal. 47, 328 (1977).

[60] M. Primet, J.M. Basset, M.V. Mathieu, and M. Prettre, J. Catal. 29, 213 (1973).